EUROPEAN ORGANIZATION FOR NUCLEAR RESEARCH

Elliptic and triangular flow of (anti)deuterons in Pb–Pb collisions at $\sqrt{s_{\mathrm{NN}}}$ = 5.02 TeV

ALICE Collaboration*

Abstract

The measurements of the (anti)deuterons elliptic flow (v_2) and the first measurements of triangular flow (v_3) in Pb–Pb collisions at a center-of-mass energy per nucleon–nucleon collisions $\sqrt{s_{\mathrm{NN}}}$ = 5.02 TeV are presented. A mass ordering at low transverse momentum (p_{T}) is observed when comparing these measurements with those of other identified hadrons, as expected from relativistic hydrodynamics. The measured (anti)deuterons v_2 lies between the predictions from the simple coalescence and blast-wave models, which provide a good description of the data only for more peripheral and for more central collisions, respectively. The mass number scaling, which is violated for v_2 is approximately valid for the (anti)deuterons v_3. The measured v_2 and v_3 are also compared with the predictions from a coalescence approach with phase-space distributions of nucleons generated by iEBE-VISHNU with AMPT initial conditions coupled with UrQMD, and from a dynamical model based on relativistic hydrodynamics coupled to the hadronic afterburner SMASH. The model predictions are consistent with the data within the uncertainties in mid-central collisions, while a deviation is observed in the most central collisions.

---

*See Appendix A for the list of collaboration members

1   Introduction

The production mechanism of light (anti)nuclei in high-energy hadronic collisions is still not fully clear and is under intense debate in the scientific community [1–5]. The understanding of the production of loosely-bound multi-baryon states in heavy-ion collisions has additional complications due to the fact that the phase transition is followed by a hadrons gas phase with intense re-scattering of hadrons. At the Large Hadron Collider (LHC) energies, the lifetime of the hadronic phase between chemical and kinetic freezeout is in the range 4–7 fm/c [6] and the kinetic freezeout temperature, when elastic interactions cease, is of the order of 100 MeV [7, 8]. The binding energy of multi-baryon systems such as light (anti)nuclei typically does not exceed a few MeV, which is almost two orders of magnitude smaller than the temperature of the system. Considering the high density of hadrons in the post-hadronization stage and the large dissociation cross sections of light (anti)nuclei, it is not clear how such loosely-bound systems can survive under these extreme conditions.

Existing phenomenological models provide very different interpretations for this observation. In the statistical hadronization model [1–3, 9, 10], light (anti)nuclei as well as all other hadron species are assumed to be emitted by a source in local thermal and hadrochemical equilibrium. Their abundances are fixed at the chemical freeze-out, occurring at a temperature of $T_{chem} = 156 \pm 4$ MeV for Pb–Pb collisions at the LHC [11]. This model provides a good description of the measured hadron yields in central nucleus–nucleus collisions [1]. However, the mechanism of hadron production and the propagation of loosely-bound states through the hadron gas phase are not addressed by this model. In the context of the statistical hadronization model, it has been conjectured that such objects could be produced at the phase transition as compact colorless quark clusters with the same quantum numbers of the final state hadrons. The survival of these states at high temperatures is interpreted as due to the low interaction cross section with the surrounding medium [1].

In the coalescence approach, multi-baryon states are assumed to be formed by the coalescence of baryons at the kinetic freeze-out. In the simplest versions of this model [12, 13], baryons are treated as point-like particles and the coalescence happens instantaneously if the momentum difference between nucleons is smaller than a given threshold, which is typically of the order of 100 MeV/c, while spatial coordinates are ignored. In the state-of-the-art implementations of the coalescence approach [4, 14], the quantum-mechanical properties of baryons and their bound states are taken into account and the coalescence probability is calculated from the overlap between the wave functions of baryons and the Wigner density of the final-state cluster. All light (anti)nuclei produced at the phase transition are assumed to be destroyed by the interactions in the hadron gas phase and regenerated with the same amount only at the latest stage of the system evolution.

To address the open question of the survival of loosely-bound multi-baryon states in the hadron gas phase with intense re-scattering, models based on relativistic hydrodynamics coupled to a hadronic afterburner have been recently developed [4, 5]. In these models, nucleons and light nuclei are produced at the phase transition using the Cooper-Frye formula [15], which describes the hadron production based on the local energy density of the fireball, and their yields are fixed to the value predicted by the thermal model at the chemical freeze-out temperature. Their propagation through the hadronic medium is simulated based on known interaction cross sections and resonant states using different transport codes. Existing calculations are based on UrQMD [16, 17], with light nuclei being produced by nucleon coalescence, and SMASH [5], where (anti)deuterons are assumed to be destroyed and regenerated with equal rates in the hadronic stage. The model based on UrQMD with nucleon coalescence [4] provides a good description of the elliptic flow of (anti)deuterons measured in Pb–Pb collisions at $\sqrt{s_{NN}} = 2.76$ TeV [18] and of that of (anti)^{3}He measured in Pb–Pb collisions at $\sqrt{s_{NN}} = 5.02$ TeV [19]. The model is able to describe the low-p_T spectra of deuterons, but over-predicts the deuterons data above 2.5 GeV/c and the (anti)^{3}He spectra in the full momentum interval. The hybrid model based on SMASH successfully describes the measured (anti)deuterons p_T-spectra and coalescence parameter B_2, defined as the ratio of the invariant

2

yield of deuterons and that of protons squared, measured in Pb–Pb collisions at $\sqrt{s_{NN}}$ = 2.76 TeV [18].

A conceptually similar approach, based on the analogy between the evolution of the early universe after the Big Bang and the space–time evolution of the system created in heavy-ion collisions, has recently been developed [20]. The production of light (anti)(hyper)nuclei in heavy-ion collisions at the LHC is considered in the framework of the Saha equation assuming that disintegration and regeneration reactions involving light nuclei proceed in relative chemical equilibrium after the chemical freeze-out of hadrons.

The existing models depict radically different pictures of the post-hadronization stage for loosely-bound states. Considering this scenario, the measurements of radial and anisotropic flow of light (anti)nuclei, i.e. the harmonics (v_n) of the Fourier decomposition of their azimuthal production distribution with respect to a symmetry plane of the collision, are relevant to study their propagation through the hadron gas phase and the dynamics of their interactions with other particles. Compared to the elliptic flow, the triangular flow of light (anti)nuclei has a better sensitivity to the fluctuating initial conditions as well as the properties of the created systems. Therefore, tighter constrains to on theoretical model that describe the production mechanism of light (anti)nuclei can be set.

The elliptic flow of (anti)deuterons was measured as a function of the transverse momentum (p_T) for different centrality classes in Pb–Pb collisions at $\sqrt{s_{NN}}$ = 2.76 TeV [18]. A clear mass ordering is observed at low p_T (p_T < 3 GeV/c) when this measurement is compared to that of other hadrons species [21], as expected from relativistic hydrodynamics. The simple coalescence model, based on the assumption that the (anti)deuterons invariant yield is proportional to the invariant yield of (anti)protons squared, is found to overestimate the measured v_2 in all centrality intervals. The data are better described by the blast-wave model, a simplified version of the relativistic hydrodynamic approach in which the collective expansion is described using a parameterized hydrodynamic flow field. The elliptic flow of (anti)^{3}He was measured in Pb–Pb collisions at $\sqrt{s_{NN}}$ = 5.02 TeV [19]. Also in the case of (anti)^{3}He, the mass ordering is observed for p_T < 3 GeV/c and the measured elliptic flow lies between the predictions of the blast-wave [22] and the simple coalescence model. A better description of the measurement is provided by a more sophisticated coalescence model where the phase-space distributions of protons and neutrons are generated by the iEBE-VISHNU hybrid model with AMPT initial conditions [4]. The picture that has emerged so far, regarding the elliptic flow of (anti)nuclei measured at LHC energies, is that the simple coalescence and blast-wave models represent the upper and lower edges of a region where the data are mostly located. Recent developments in the coalescence approach, which take into account momentum-space correlations of nucleons and their quantum-mechanical properties, provide a better description of the data [4, 5].

In this paper, a precision measurement of the (anti)deuterons elliptic flow and first ever measurement of (anti)deuterons triangular flow for different p_T and centrality intervals in Pb–Pb collisions at $\sqrt{s_{NN}}$ = 5.02 TeV are presented. Thanks to the large data sample collected at higher energy, the elliptic flow measurement is performed in wider p_T and up to a higher centrality intervals compared to that in Pb–Pb collisions at $\sqrt{s_{NN}}$ = 2.76 TeV, allowing for a more differential comparison with the theoretical models.

2   The ALICE detector

A detailed description of the ALICE detector can be found in [23] and references therein. The main sub-detectors used for the present analysis are the V0 detector, the Inner Tracking System (ITS), the Time Projection Chamber (TPC), and the Time-of-Flight detector (TOF), which are located inside a solenoidal magnet that provides a uniform field of 0.5 T directed along the beam direction. The V0 detector [24] consists of two arrays of scintillation counters placed around the beam vacuum tube on either side of the interaction point: one covering the pseudorapidity interval 2.8 < η < 5.1 (V0A) and the other one covering −3.7 < η < −1.7 (V0C). Each V0 array consists of four rings in the radial direction, with each ring comprising eight cells with the same azimuthal size. The scintillator arrays have an intrinsic time

resolution better than 0.5 ns, and their timing information is used in coincidence for offline rejection of events produced by the interaction of the beams with residual gas in the vacuum pipe. The V0 scintillators are used to determine the collision centrality from the measured charged-particle multiplicity [25–27] and to measure the orientation of the symmetry plane of the collision.

The ITS [28], designed to provide high-resolution track points in the vicinity of the nominal vertex position, is composed of three subsystems of silicon detectors placed around the interaction region with a cylindrical symmetry. The Silicon Pixel Detector (SPD) is the subsystem closest to the beam vacuum tube and it is made of two layers of pixel detectors. The third and the fourth layers are formed by Silicon Drift Detectors (SDD), while the outermost two layers are equipped with double-sided Silicon Strip Detectors (SSD). The ITS covers the pseudorapidity interval $|\eta| < 0.9$.

The same pseudorapidity interval is covered by the TPC, which is the main tracking detector, consisting of a hollow cylinder whose axis coincides with the nominal beam axis.

The active volume of 90 m^3 is filled with a gas mixture containing 88% Ar and 12% CO_2.

The trajectory of a charged particle is estimated using up to 159 space points. The charged-particle tracks are then built by combining the hits in the ITS and the reconstructed space points in the TPC. The TPC is also used for particle identification (PID) by measuring the specific energy loss (dE/dx) in the TPC gas.

The TOF detector [29] covers the full azimuth in the pseudorapidity interval $|\eta| < 0.9$. The detector is based on the Multi-gap Resistive Plate Chambers (MRPCs) technology and it is located, with a cylindrical symmetry, at an average radial distance of 380 cm from the beam axis. The TOF allows for PID, based on the difference between the measured time-of-flight and its expected value, computed for each mass hypothesis from the track momentum and length. The resolution on the measurement of the time-of-flight is about 60 ps in heavy-ion collisions.

3 Data sample and analysis techniques

3.1 Event and track selections

The data sample used for the measurements presented in this paper was recorded by ALICE in 2015 during the LHC Pb–Pb run at $\sqrt{s_{NN}}$ = 5.02 TeV. A minimum bias trigger was used during the data taking, which required coincident signals in both V0 detectors. An offline event selection is applied to remove beam-gas collisions using the timing information provided by the V0 detectors and the Zero-Degree Calorimeters [23]. Events with multiple primary vertices identified with the SPD are tagged as pileup and removed from the analysis. In addition, events with significantly different charged-particle multiplicities measured by the V0 detector and by the tracking detectors at midrapidity, which have different readout times, are rejected. After the offline event selection, the remaining contribution of beam-gas events is smaller than 0.02% [23] and the fraction of pileup events is found to be negligible. The primary vertex position is determined from tracks reconstructed in the ITS and TPC as described in [23] and only events with a reconstructed primary vertex position along the beam axis within 10 cm from the from the nominal interaction point are selected. The total number of events selected for the analysis for centrality 0–70% is about 73 million.

Deuteron (d) and antideuteron ($\bar{\text{d}}$) candidates are selected from charged-particle tracks reconstructed in the ITS and TPC in the kinematic range $|\eta| < 0.8$ and $0.8 < p_T < 6$ GeV/c. Only tracks with at least 70 clusters out of a maximum of 159 and with a χ^2 per degree-of-freedom for the track fit lower than 2 are accepted. In addition, in order to guarantee a track-momentum resolution of 2% in the measured p_T range and a dE/dx resolution of about 6%, each track is required to be reconstructed from at least 80% of the number of expected TPC clusters and to have at least one hit in either of the two innermost layers of the ITS. The distances of closest approach (DCA) to the primary vertex in the

plane perpendicular and parallel to the beam axis for the selected tracks are determined with a resolution better than 300 μm [23]. To suppress the contribution of secondary particles, the reconstructed tracks are required to have a longitudinal DCA smaller than 2 cm and a transverse DCA smaller than $0.0105 + 0.0350/p_T^{1.1}$ cm, with p_T in units of GeV/c. The latter corresponds to approximately $7\sigma_{DCA}(p_T)$, where $\sigma_{DCA}(p_T)$ is the transverse DCA resolution in the corresponding p_T interval.

3.2 (Anti)deuterons identification

The (anti)deuterons identification technique used in this analysis is similar to that used in the previous measurement in Pb–Pb collisions at $\sqrt{s_{NN}}$ = 2.76 TeV [18]. For transverse momenta up to 1.4 GeV/c (anti)deuterons are identified using the only the TPC information by requiring that the average dE/dx is within 3σ from the expected average value for the (anti)deuteron mass hypothesis. For $p_T > 1.4$ GeV/c the 3σ TPC identification is complemented by the signal provided by the TOF detector. The number of (anti)deuterons in each p_T interval is extracted from a fit of the $\Delta M = m_{TOF} - m_{d_{pdg}}$, where m_{TOF} is the particle mass calculated using the time-of-flight measured by the TOF and $m_{d_{pdg}}$ is the nominal mass of deuterons taken from [30]. In the left panel of Fig. 1 the ΔM distribution for (anti)deuterons with $2.2 \leq p_T < 2.4$ GeV/c in the centrality interval 20–30%, is shown. The d+$\overline{\text{d}}$ signal is fitted using a Gaussian with an exponential tail, while the background, originating from TOF hits incorrectly associated to tracks extrapolated from the TPC, is modeled with an exponential function.

Deuterons and antideuterons are summed together ($\overline{\text{d}}$+d) in all the centrality intervals and for p_T larger than 1.4 GeV/c. This is possible since the v_2 and v_3 measured for v_2 and v_3 for d and $\overline{\text{d}}$ are consistent within the statistical uncertainties. At lower p_T, deuterons produced by spallation in interactions between particles and the detector material or in the beam vacuum tube constitute a significant background. For this reason, for $p_T < 1.4$ GeV/c only antideuterons, which are not affected by this background, are used in the analysis. Since no difference is expected for the v_2 and v_3 of $\overline{\text{d}}$ and d, hereafter deuterons will denote results for antideuteron for $p_T < 1.4$ GeV/c and the sum of d and $\overline{\text{d}}$ elsewhere. The contribution of secondary deuterons produced in weak decays of hypertritons is negligible considering that the production rate of (hyper)nuclei with mass number $A = 3$ is suppressed compared to that of $A = 2$ by a factor of approximately 300 in Pb–Pb collisions at $\sqrt{s_{NN}}$ = 2.76 TeV [31]. A similar suppression is expected in Pb–Pb collisions at $\sqrt{s_{NN}}$ = 5.02 TeV.

3.3 Flow analysis techniques

The particle azimuthal distribution of charged particles with respect to the n-th order flow symmetry plane Ψ_n [32–35] can be expressed as a Fourier series

$$E\frac{\text{d}^3N}{\text{d}p^3} = \frac{1}{2\pi}\frac{\text{d}^2N}{p_T\text{d}p_T\text{d}y}\left(1 + \sum_{n=1}^{\infty} 2v_n \cos\left(n\left(\varphi - \Psi_n\right)\right)\right), \tag{1}$$

where E is the energy of the particle, p the momentum, φ the azimuthal angle, y the rapidity, and

$$v_n = \langle\cos\left(n(\varphi - \Psi_n)\right)\rangle. \tag{2}$$

The second coefficient of the Fourier series (v_2) is called elliptic flow and is related to the initial geometrical anisotropy of the overlap region of the colliding nuclei. The third-order flow coefficient (v_3), called triangular flow, is generated by fluctuations in the initial distribution of nucleons and gluons in the overlap region [34, 36, 37]. The same fluctuations are responsible for the v_2 measured in most central collisions (centrality < 5%) [38]. The v_n coefficients are measured using the Scalar Product (SP) method [32, 39]. This is a two-particle correlation technique based on the scalar product of the unit flow vector of the particle of interest, k, and the Q-vector. The unit flow vector is denoted by $\mathbf{u}_{n,k} = \exp(in\varphi_k)$, where φ_k is the azimuthal angle of the particle k.

The Q-vector is computed from a set of reference flow particles and is defined as:

$$\mathbf{Q}_n = \sum w_i e^{in\varphi_i} \tag{3}$$

where, in general, φ_i is the azimuthal angle for the i-th reference flow particle, n is the order of the harmonic, and w_i is a weight applied to correct for reference flow.

The v_n flow coefficients are calculated as

$$v_n\{\text{SP}\} = \frac{\langle\langle \mathbf{u}_{n,k}\mathbf{Q}_n^*\rangle\rangle}{\sqrt{\frac{\langle\mathbf{Q}_n\mathbf{Q}_n^{A*}\rangle\langle\mathbf{Q}_n\mathbf{Q}_n^{B*}\rangle}{\langle\mathbf{Q}_n^A\mathbf{Q}_n^{B*}\rangle}}}. \tag{4}$$

Single brackets $\langle...\rangle$ denote an average over all events, while double brackets $\langle\langle...\rangle\rangle$ indicate an average over all particles in all events, and $*$ denotes the complex conjugate. The denominator is a correction factor that is introduced to take into account the resolution of the $\mathbf{Q}_n$ vector. In this analysis, the $\mathbf{Q}_n$ vector is calculated from the azimuthal distribution of the energy deposition measured in the V0A, while the $\mathbf{Q}_n^A$ and $\mathbf{Q}_n^B$ vectors are determined from the azimuthal distribution of the energy deposited in the V0C and the azimuthal distribution of tracks reconstructed in the TPC, respectively. Using these detectors, a pseudorapidity gap $|\Delta\eta| > 2$ between the particle of interest and the reference flow particles is introduced. Such a pseudorapidity gap reduces non-flow effects, which are correlations not arising from the collective expansion of the system (e.g. resonances decays and jets).

The purity of the sample of deuterons identified using the TPC in the $0.8 < p_T < 1.4$ GeV/c interval is around 100%. In this transverse momentum interval the v_2 and v_3 coefficients were evaluated on a track-by-track basis and then averaged in each p_T interval. For higher p_T, the v_n coefficients are calculated in different ranges of ΔM. The $v_n(\Delta M)$ contains contributions from the signal (v_n^{sig}) and from the background (v_n^{bkg})

$$v_n(\Delta M) = v_n^{\text{sig}}\frac{N^{\text{sig}}}{N^{\text{tot}}}(\Delta M) + v_n^{\text{bkg}}(\Delta M)\frac{N^{\text{bkg}}}{N^{\text{tot}}}(\Delta M), \tag{5}$$

where N^{sig} is the number of deuterons, N^{bkg} the number of background particles and N^{tot} is their sum. The signal v_n is extracted from a fit to the observed v_n as a function of ΔM, in which v_n^{bkg} is described using a first-order polynomial function, and v_n^{sig} is a free fit parameter. N^{sig} and N^{bkg} are obtained from the fit to the ΔM distribution using a Gaussian with an exponential tail for the signal and an exponential for the background. The signal extraction procedure is illustrated in Fig. 1 for $2.2 \leq p_T < 2.4$ GeV/c ($2.0 \leq p_T < 2.4$ GeV/c for v_3) in the centrality interval 20–30%.

The elliptic and triangular flow of deuterons are measured in centrality intervals of 5% width and then the results in wider centrality intervals are obtained as weighted averages of these measurements using the number of deuteron candidates, in the same centrality interval of 5% width as a weight, similarly to what was performed in [19].

3.4 Systematic uncertainties

The sources of systematic uncertainties for the elliptic and triangular flow of deuterons are related to event selection, tracking, (anti-)deuterons identification, and the technique used for the signal extraction. The contribution related to the event selection is estimated by taking into account the differences in the v_2 and v_3 measurements obtained using different event-selection criteria. In particular, the fiducial region for the vertex position along the beam axis is varied from the range $[-10, 10]$ cm to $[-7, 7]$ cm to probe the magnitude of potential edge effects. To investigate possible effects due to charge asymmetries during tracking and geometrical asymmetries in the detector, the differences between the results obtained by
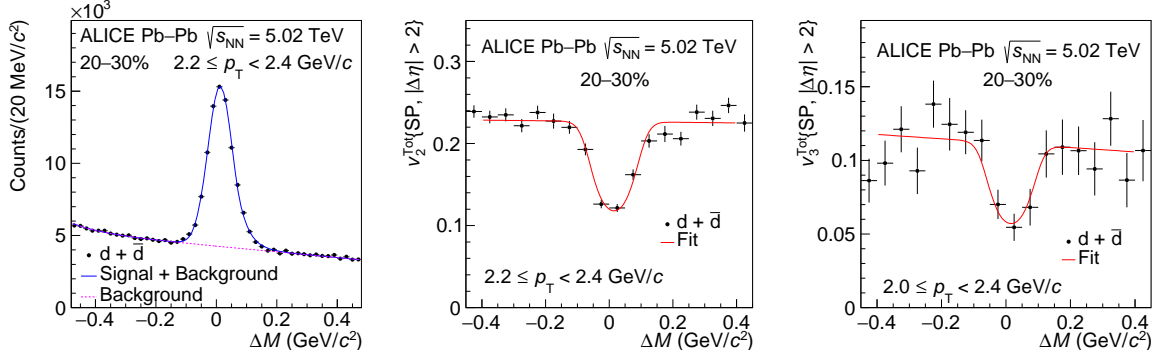
Figure 1: (Color online) Raw yield (left), v_2 (middle) and v_3 (right) of d+$\bar{\mathrm{d}}$ candidates as a function of ΔM for $2.2 \leq p_{\mathrm{T}} < 2.4$ GeV/c ($2.0 \leq p_{\mathrm{T}} < 2.4$ GeV/c for v_3) and in the centrality interval 20–30%. The data points represent the measurements. The curve on the left panel is the total fit (signal plus background) as described in the text. The curves in the middle and right panel are the fits performed using Eq. 5. Vertical bars represent the statistical uncertainties.

using opposite magnetic field polarities are included. Analogously, the default centrality estimator is changed to that based on the number of hits in the first or second layer of the ITS. Finally, the effect related to pileup rejection is tested by requiring a stronger correlation between the V0 and central barrel multiplicities. These contributions are assumed to be independent and added in quadrature. The total systematic uncertainty due to event selection is found to be around 1.5% for both v_2 and v_3.

To estimate the systematic uncertainties due to reconstruction and identification of deuterons, the track selection and the TPC PID criteria are varied with respect to the default choice and the v_n measurements are repeated for each of these different settings. The RMS of the distribution of v_n measurements in each p_{T} interval is considered as systematic uncertainty. To minimize the effect of statistical fluctuations, all variations smaller than $2\sqrt{\left|\sigma_0^2 - \sigma_i^2\right|}$ are not included in the estimate of the systematic uncertainties [40], where σ_0 is the statistical uncertainty of the default value while σ_i is that corresponding to the ith selection criterion. The probability distribution for the variations of data points due to systematic effects related to tracking and PID is assumed to be uniform in each p_{T} interval and the difference between the maximum and minimum value divided by $\sqrt{12}$ is assigned as systematic uncertainty. This contribution ranges from 1% and 3% depending on p_{T} and centrality.

To estimate the contribution to the systematic uncertainties due to the signal extraction, the function used to describe the v_n^{bkg} is changed. In addition to a first-order polynomial, a constant function and a second-order polynomial are also used, and the maximum difference with respect to the default measurement is considered as systematic uncertainty. A contribution up to 5% is observed for central collisions and for $p_{\mathrm{T}} < 2$ GeV/c. Moreover, different functions and fitting ranges are used to describe the signal and the background of Eq. 5. More specifically, besides a Gaussian function with an exponential tail, a Gaussian is also used for the signal, while single and double exponential, and linear functions are also used for the background. This contribution is relevant only for $p_{\mathrm{T}} > 1.4$ GeV/c, where the TOF is used to extract the signal, and is found to vary from 1% to 6% depending on p_{T} and centrality. Table 1 shows the summary of the different contributions to the systematic uncertainties for the v_2 and v_3 of deuterons. The total uncertainties are given by their sum in quadrature, assuming that all contributions are independent.

4 Results and discussion

The v_2 and v_3 of deuterons measured in Pb–Pb collisions at $\sqrt{s_{\mathrm{NN}}} = 5.02$ TeV are shown in Fig. 2 as a function of p_{T} for different centrality intervals. In the measured p_{T} interval, an increasing trend is observed with increasing p_{T} and going from central to more peripheral Pb–Pb collisions, as expected based on the relativistic hydrodynamic description of the collective expansion of a hot and dense medium [41].

Table 1: Summary of the systematic uncertainties for the deuterons v_2 and v_3. The maximum deviation of the systematic uncertainty is reported.

Source	Value	
	v_2	v_3
Event selections	1.5%	1.5%
Tracking and particle identification	1–3%	1–2%
Signal extraction	1–4%	2–6%
Total	2–7%	3–7%

Initial state fluctuations of the energy density distribution of partons in the colliding nuclei imply a non-zero v_3 [37].

The measurement presented in this paper shows that these initial state effects, already observed for other hadron species at LHC energies [42, 43], are also visible for deuterons.
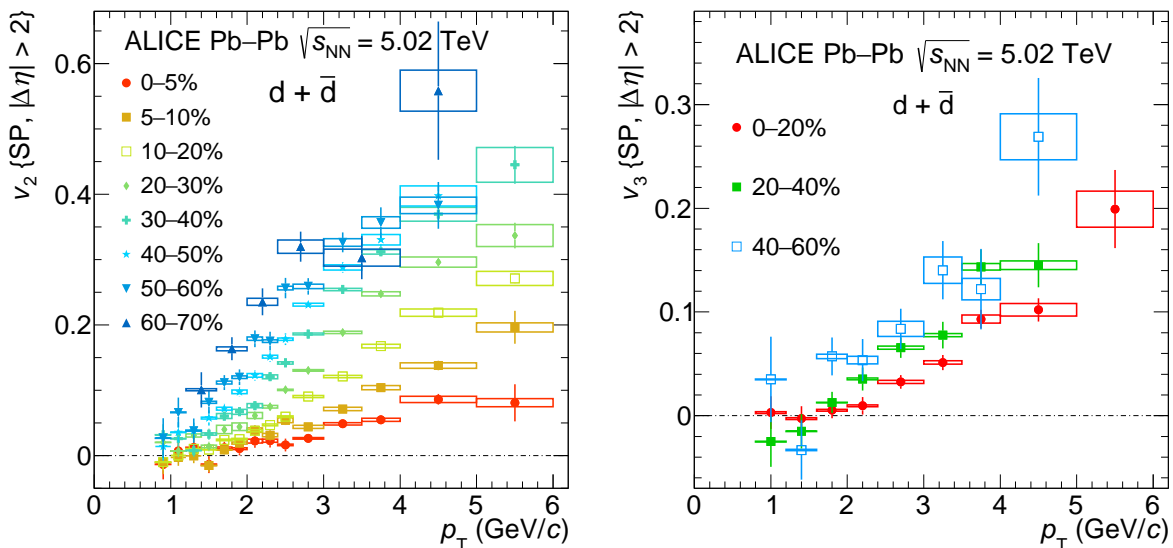
Figure 2: (Color online) Elliptic (v_2, left) and triangular (v_3, right) flow of deuterons as a function of p_T for different centrality intervals measured in Pb–Pb collisions at $\sqrt{s_{NN}}$ = 5.02 TeV. The horizontal line at zero is to guide the eye. Vertical bars and boxes represent the statistical and systematic uncertainties, respectively.

The measurement of the deuterons v_2 in Pb–Pb collisions at $\sqrt{s_{NN}}$ = 5.02 TeV is compared to that in Pb–Pb collisions at $\sqrt{s_{NN}}$ = 2.76 TeV [18] in Fig. 3 for two centrality intervals. The observed v_2 and their trend are similar at the two center-of-mass energies, but a decrease of the observed elliptic flow for a given p_T is observed with increasing center-of-mass energy. This effect is more pronounced in peripheral rather than in central collisions. A similar effect was observed for the proton v_2 measurements [43] and is interpreted as partially due to the increasing radial flow with increasing collision energy, which produces a shift of the v_2 towards higher p_T.

The effect due to radial flow is assessed quantitatively by comparing the ratio of the deuteron and proton v_2 as a function of p_T at the two energies. The ratio between the deuteron v_2 in Pb–Pb collisions at $\sqrt{s_{NN}}$ = 5.02 TeV to that measured at $\sqrt{s_{NN}}$ = 2.76 TeV, with v_2 and p_T scaled by the mass number $A = 2$, is shown in Fig. 4 for two centrality intervals in comparison with the same ratio for protons. As indicated by these ratios, the radial flow effects are quantitatively very similar for protons and deuterons. It has to be noted that a mass scaling would lead to the same conclusion since the binding energy of
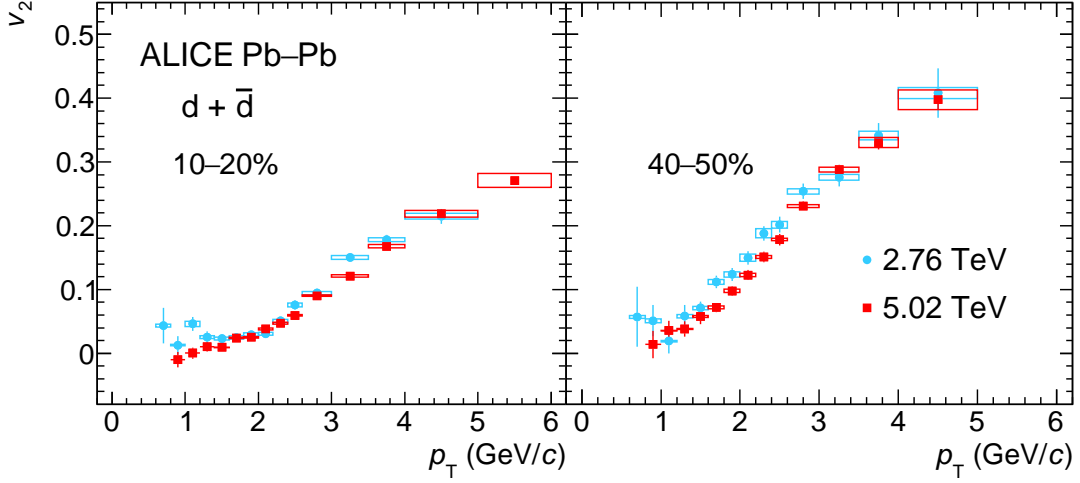
Figure 3: (Color online) Deuterons v_2 measured in Pb–Pb collisions at $\sqrt{s_{NN}}$ = 5.02 TeV (red square) compared to that measured at $\sqrt{s_{NN}}$ = 2.76 TeV [18] (light blue circles) for two centrality intervals (10–20% and 40–50%). Both protons and deuteron elliptic flow were measured for pseudorapidity gap between the particle of interest and the reference flow particle $|\Delta\eta| > 0.9$. Vertical bars and boxes represent the statistical and systematic uncertainties, respectively.

deuteron is of 2.2 MeV, i.e. the deuteron mass is approximately equal to $2m_p$, where m_p is the proton mass.
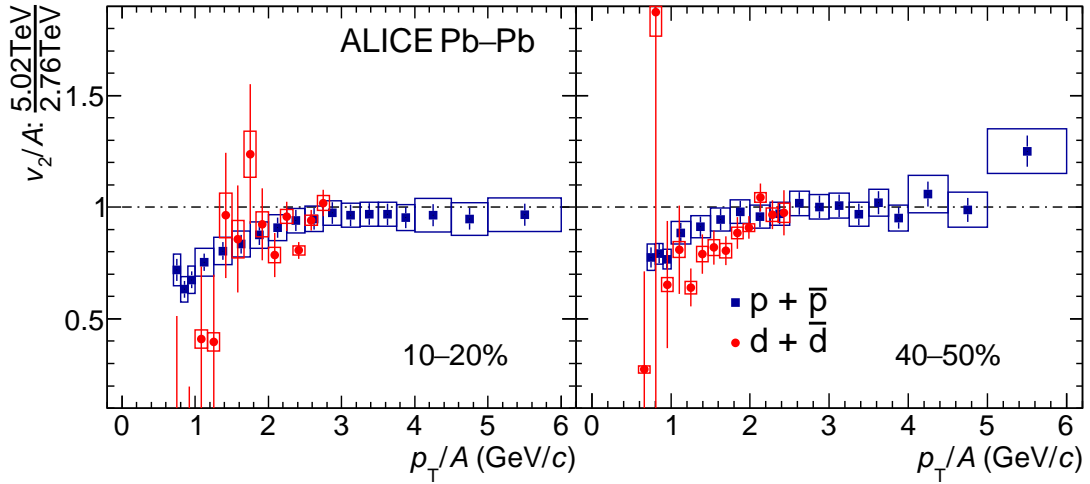
Figure 4: (Color online) Ratio of the v_2 of deuterons measured in Pb–Pb collisions at $\sqrt{s_{NN}}$ = 5.02 TeV to that measured at $\sqrt{s_{NN}}$ = 2.76 TeV (red circles) compared with the same ratio obtained for protons (blue squares) for two centrality intervals (10–20% on the left panel and 40–50% on the right panel). For a direct comparison of protons and deuterons, the measured v_2 and p_T have were divided by A. Vertical bars and boxes represent the statistical and systematic uncertainties, respectively.

The elliptic flow of deuterons is compared to that of pions, kaons, protons and (anti)^{3}He measured at the same center-of-mass energy [19, 43] in Fig. 5. Since the (anti)^{3}He elliptic flow is measured in centrality intervals of 20% width due to its rarer production compared to that of lighter hadrons, the v_2 of pions, kaons, protons and deuterons are re-calculated to match the same centrality intervals. This is achieved

by averaging the v_2 measurements of these particles in narrower centrality intervals weighted by the corresponding p_T spectra [8, 44]. A clear mass ordering of v_2 is observed at low p_T, as expected for a system expansion driven by the pressure gradient as described by relativistic hydrodynamics [41, 45, 46].
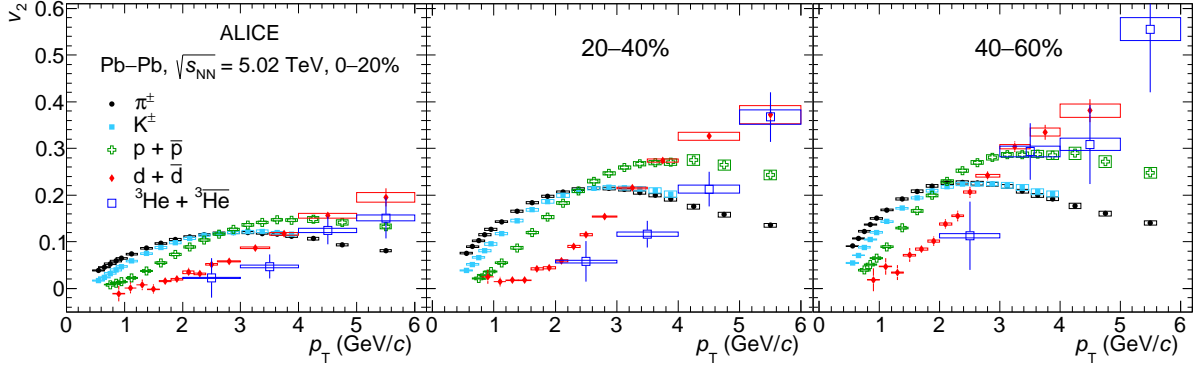
Figure 5: (Color online) Comparison of the elliptic flow of pions, kaons, protons, deuterons and (anti)^{3}He in different centrality intervals for Pb–Pb collisions at $\sqrt{s_{NN}}$ = 5.02 TeV. (Anti)^{3}He v_2 is measured using the Event Plane method [19]. Vertical bars and boxes represent the statistical and systematic uncertainties, respectively.

In Fig. 6, the deuterons v_3 is compared to that of pions, kaons, and protons at the same center-of-mass energy [43] for the centrality intervals 0–20% (left) and 20–40% (right). Also for the v_3, a clear mass ordering is observed for $p_T \lesssim 2.5$ GeV/c and $p_T \lesssim 3$ GeV/c for the centrality intervals 0–20% and 20–40%, respectively.
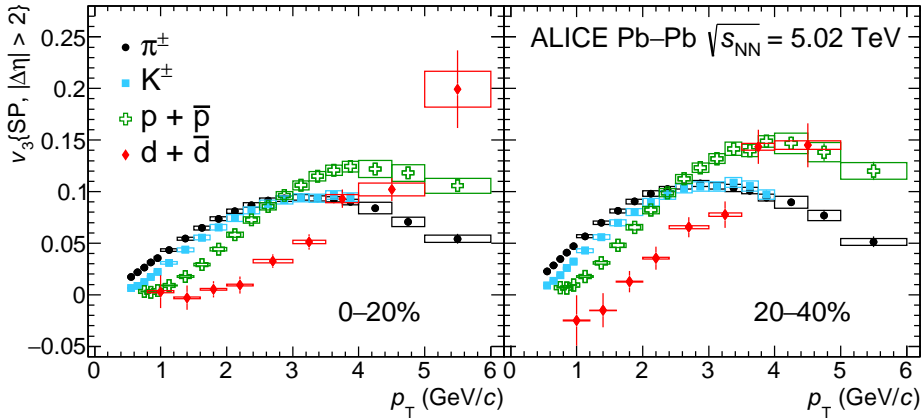
Figure 6: (Color online) Triangular flow (v_3) of deuterons, pions, kaons, and protons [43] as a function of p_T for the centrality intervals 0–20% and 20–40%. Vertical bars and boxes represent the statistical and systematic uncertainties, respectively.

4.1 Comparison with the blast-wave model predictions

The elliptic flow of deuterons is compared with the expectations of the blast-wave model [22, 47, 48], which is based on the assumption that the system produced in heavy-ion collisions is locally thermalized and expands collectively with a common velocity field. The system is assumed to undergo an instantaneous kinetic freeze-out at the temperature T_{kin} and to be characterized by a common transverse radial flow velocity at the freeze-out surface. A simultaneous fit of the v_2 and the p_T spectra of pions, kaons, and protons [8, 43] with the blast-wave model is performed in the transverse-momentum ranges

$0.5 \leq p_T^{\pi} < 1$ GeV/c, $0.7 \leq p_T^{K} < 2$ GeV/c, and $0.7 \leq p_T^{p} < 2.5$ GeV/c. The four free parameters of the blast-wave function are the kinetic freeze-out temperature (T_{kin}), the variation in the azimuthal density of the source (s_2), the mean transverse expansion rapidity (ρ_0), and the amplitude of its azimuthal variation (ρ_a), as described in [47]. The values of these parameters extracted from the fits are reported in Table 2 for each centrality interval. These values are employed to predict the elliptic flow of deuterons under the assumption that the same kinetic freeze-out conditions apply for all particles produced in the collision. The deuteron mass is taken from [30].

Table 2: Blast-wave parameters extracted from the simultaneous fits of the p_T spectra and v_2 of pions, kaons, and protons measured at $\sqrt{s_{NN}}$ = 5.02 TeV. See text for details. The error assigned to each parameter is shown only with one significant digit.

Centrality	Fit parameters			
	T_{kin} (MeV)	s_2 (10^{-2})	ρ_0 (10^{-1})	ρ_a (10^{-2})
0–5%	104 ± 1	2.63 ± 0.01	8.57 ± 0.01	0.83 ± 0.01
5–10%	106 ± 1	4.15 ± 0.01	8.85 ± 0.01	1.47 ± 0.01
10–20%	107 ± 1	6.09 ± 0.01	9.12 ± 0.01	2.17 ± 0.01
20–30%	109 ± 1	8.25 ± 0.01	9.02 ± 0.01	2.85 ± 0.01
30–40%	111 ± 1	10.1 ± 0.01	8.61 ± 0.01	3.25 ± 0.01
40–50%	116 ± 1	12.3 ± 0.01	7.73 ± 0.01	3.30 ± 0.01
50–60%	121 ± 1	14.5 ± 0.01	6.93 ± 0.01	2.85 ± 0.01
60–70%	129 ± 1	17.4 ± 0.01	5.95 ± 0.01	1.74 ± 0.01

The blast-wave fits to the v_2 of pions, kaons, and protons and the predictions for the deuterons v_2 are reported in Fig. 7 for the centrality intervals 10–20% and 40–50%. In the lower panels, the data-to-fit ratios for pions, kaons, and protons and the ratios of the deuterons v_2 to the model are shown. Because of the finite size of the p_T intervals, the average of the blast-wave function within the interval, weighted by the p_T spectrum of the corresponding particle species, is considered in the calculation of these ratios.

The predictions of the blast-wave model underestimate the deuterons elliptic flow experimental values in semi-peripheral collisions for $p_T > 1.4$ GeV/c, while they are close to the measurements for central events in the measured p_T interval. This is better observed in Fig. 8, which shows the centrality evolution of the data-to-model ratios.

4.2 Test of the coalescence hypothesis

The deuterons v_2 and v_3 are compared to the expectations of a coalescence approach based on mass number scaling and isospin symmetry, for which the proton and neutron v_2 (v_3) are identical. In particular, the v_2 (v_3) measured for protons [43] was used to predict the v_2 (v_3) of deuterons using the following relation [49]

$$v_{2(3),d}(p_T) = \frac{2v_{2(3),p}(p_T/2)}{1 + 2v_{2(3),p}^2(p_T/2)}. \tag{6}$$

The results of this calculation for different centrality intervals for v_2 are shown in the left panel of Fig. 9. The measured elliptic flow in 10–20% and 40–50% centrality intervals of deuterons is compared with coalescence model predictions from Eq. 6 using the measured v_n of protons. Similarly, the right panel of Fig. 9 shows a comparison between the calculated and measured v_3 in the 0–20% and 20–40% centrality intervals.

The coalescence model overestimates the deuteron v_2 by about 20% to 30% in central collisions and is close to the data for semi-peripheral collisions, as illustrated in Fig. 10 which shows the centrality
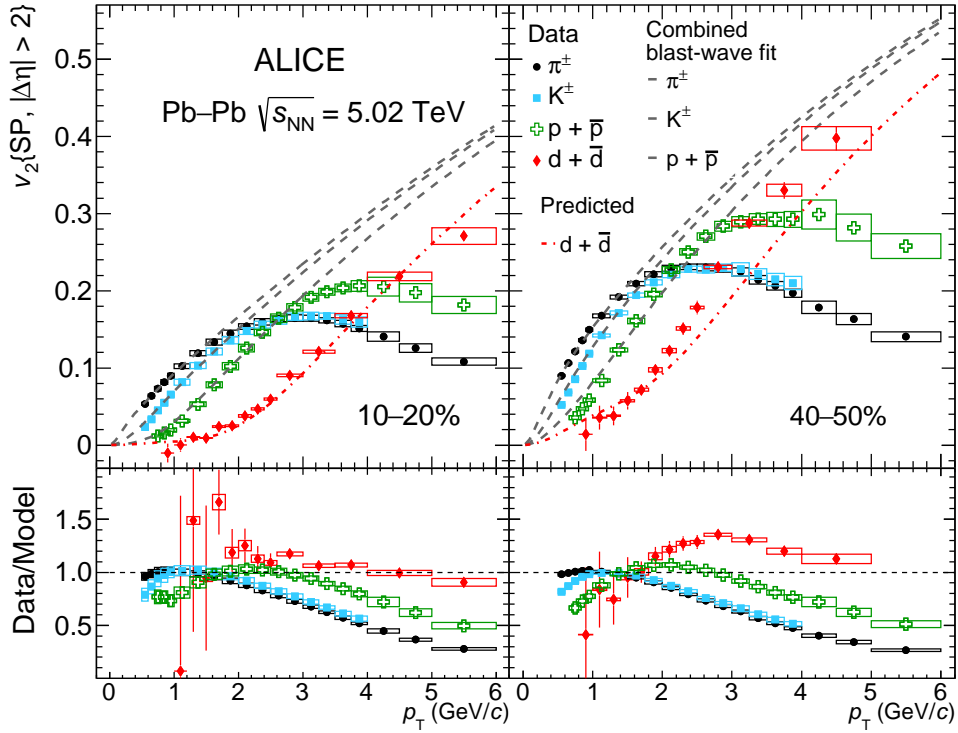
Figure 7: (Color online) Blast-wave fits to the v_2 (p_T) of pions, kaons, and protons [43] and predictions of the deuterons v_2 (p_T) for the centrality intervals 10–20% (left) and 40–50% (right). In the lower panels, the data-to-fit ratios are shown for pions, kaons, and protons as well as the ratio of the deuterons v_2 to the blast-wave predictions. Vertical bars and boxes sent the statistical and systematic uncertainties, respectively. The dashed line at one is to guide the eye.
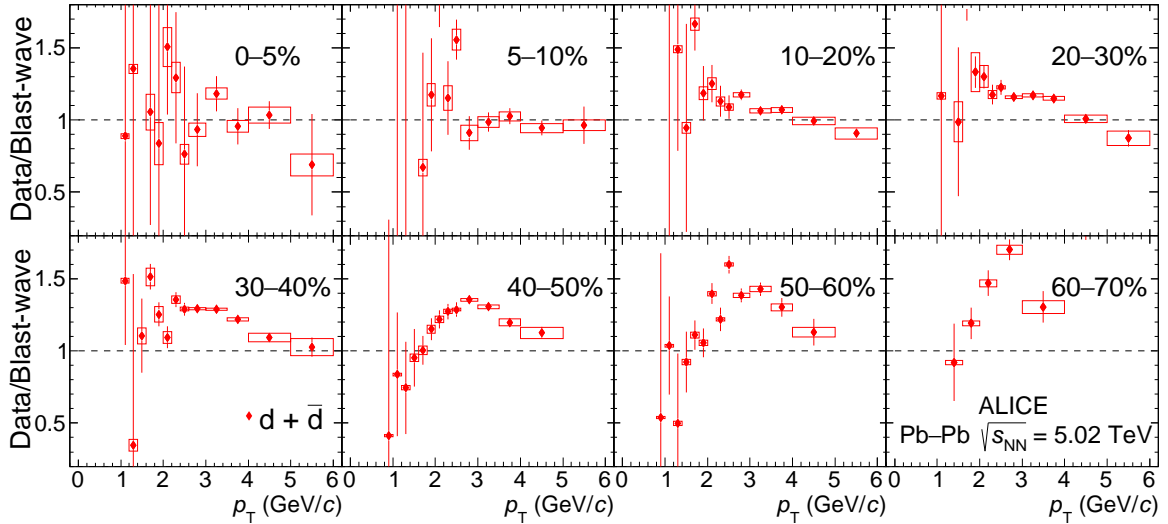

Figure 8: (Color online) Data-to-model ratios of the deuterons v_2 to the blast-wave predictions as a function of p_T for different centrality intervals as indicated in each pad. Vertical bars and boxes represent the statistical and systematic uncertainties, respectively.

evolution of the data-to-model ratio. The coalescence approach seems to have a slightly better agreement
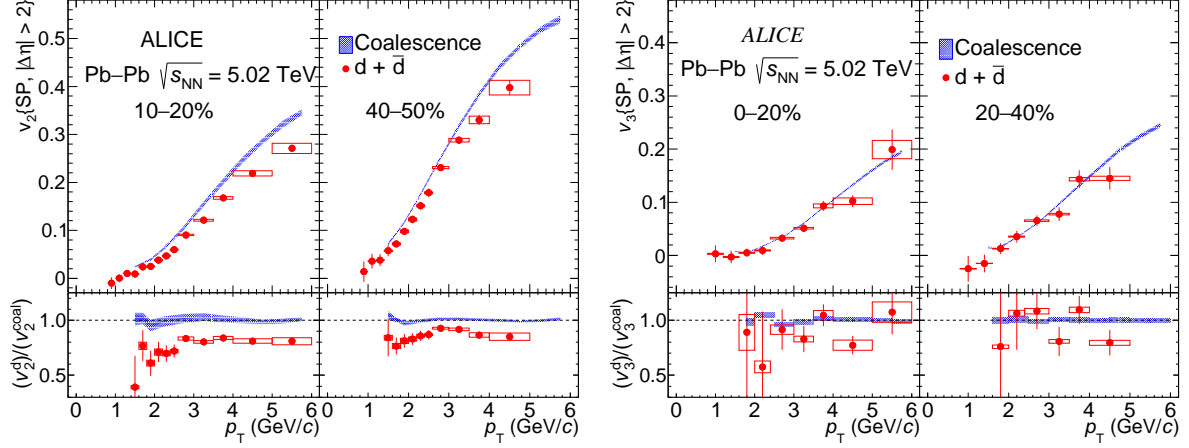
Figure 9: (Color online) Measured deuterons v_2 and v_3 (red circles) compared with the expectations from simple coalescence (Eq. 6) (blue shaded bands) for two centrality intervals. In the left panel, the v_2 measurements in the 10–20% and 40–50% centrality intervals is shown. The right panel displays the results of v_3 in the 0–20% and 20–40% centrality intervals. The bottom panels show the ratio between the measured v_2 (v_3) and the expectations from the coalescence model. In each panel, vertical bars and boxes represent the statistical and systematic uncertainties, respectively. The line at one is to guide the eye.

with deuterons v_3; however, the large statistical uncertainties on the v_3 measurements do not allow for conclusive statements.
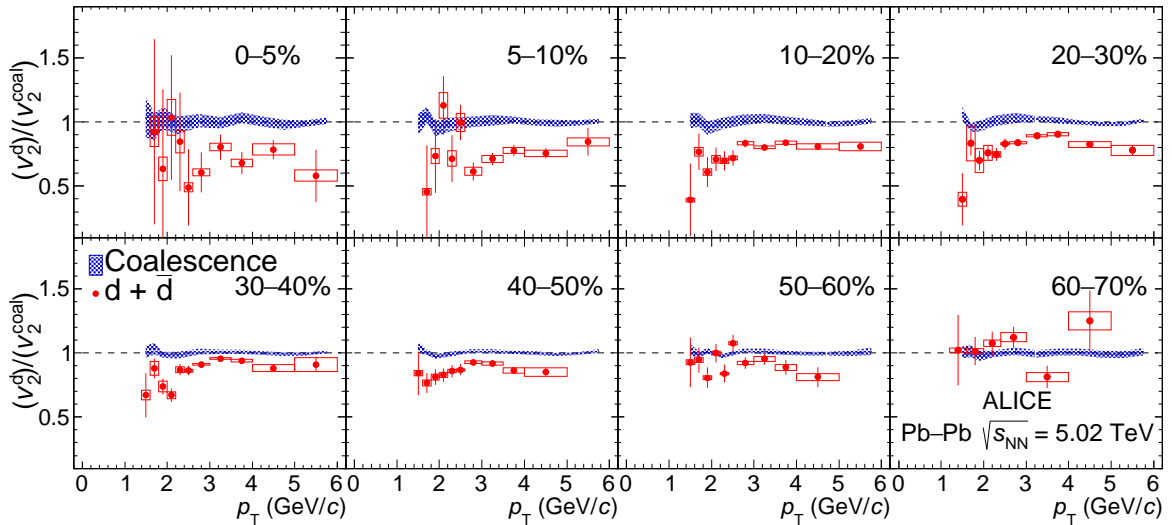
Figure 10: (Color online) Centrality evolution of the deuterons v_2 compared with the expectations from simple coalescence model (Eq. 6). Vertical bars and boxes represent the statistical and systematic uncertainties, respectively.

4.3 Comparison with iEBE-VISHNU and coalescence calculations

In Fig. 11, the deuterons v_2 and v_3 are compared to a model [4] implementing light nuclei formation via coalescence of nucleons originating from a hydrodynamical evolution of the fireball coupled to an UrQMD simulation of the hadronic cascade [16, 17]. In this model, the coalescence probability is calculated as the superposition of the wave functions of protons and neutrons and the Wigner function of

the deuterons. The coalescence happens in a flowing medium introducing position-momentum correlations, which are absent in the simple coalescence approach. The phase-space distributions of protons and neutrons are generated from the iEBE-VISHNU hybrid model with AMPT [50] initial conditions. This model provides a good description of the protons spectra up to 3 GeV/c and of the deuterons v_2 measured in Pb–Pb collisions at $\sqrt{s_{NN}}$ = 2.76 TeV [4]. The predictions are consistent with the measured deuterons v_2 for events with centrality larger than 20% and for measured v_3 within the statistical and systematical uncertainties, while some discrepancy at the level of 2σ (taking into account statistical and systematical uncertainties in quadrature) are observed for for the centrality interval 10–20% as shown in Fig. 11.
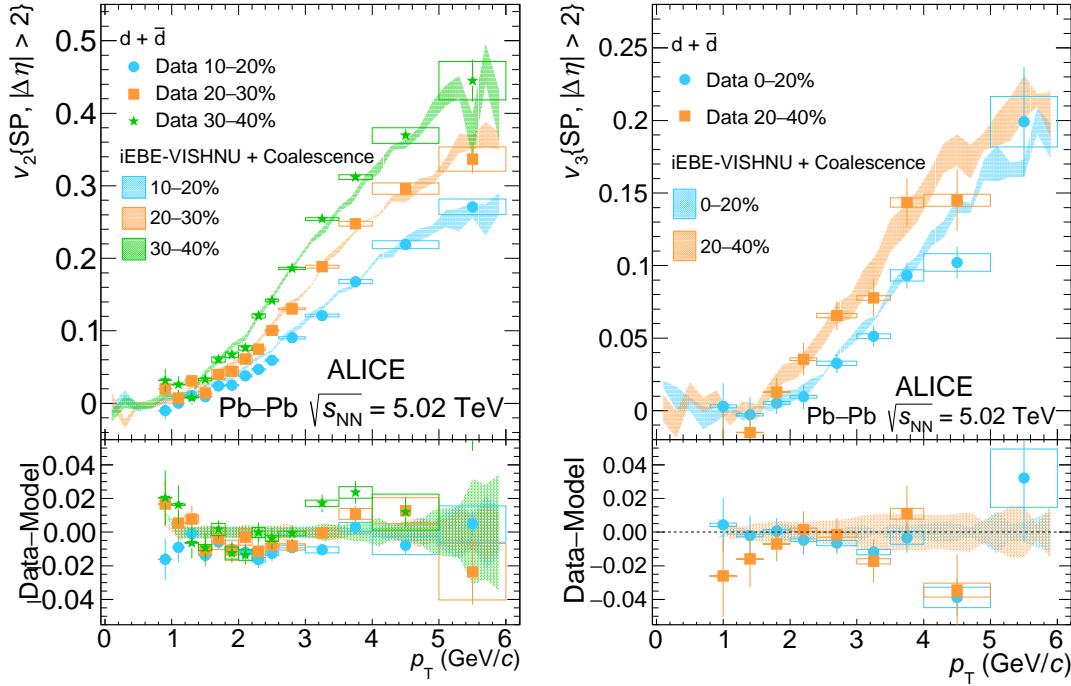
Figure 11: Elliptic (left) and triangular (right) flow of deuterons compared to the predictions iEBE-VISHNU hybrid model with AMPT initial conditions [4]. The predictions are shown as bands whose widths represent the statistical uncertainties associated with the model. The data-to-model differences are shown in the lower panels. Vertical bars and boxes represent the statistical and systematic uncertainties, respectively.

4.4 Comparison with a hybrid (hydrodynamics + transport) approach expectations

The deuterons v_2 measured in the centrality intervals 10–20%, 20–30%, and 30–40% is compared in Fig. 12 with the predictions from a hybrid model based on relativistic viscous hydrodynamics, with fluctuating initial conditions generated by T$_R$ENTo [51], coupled to the hadronic afterburner SMASH [5]. The simulations are obtained by using the JETSCAPE 1.0 event generator [52]. The parameters of this model, including the shear and bulk viscosities, are tuned to the measurements of p_T spectra and azimuthal flow of pions, kaons, and protons obtained by ALICE in Pb–Pb collisions at $\sqrt{s_{NN}}$ = 2.76 TeV [7, 21] and by PHENIX and STAR in Au–Au collisions at $\sqrt{s_{NN}}$ = 200 GeV [53–55]. The interactions of deuterons with other hadrons in the hadron gas phase are simulated using SMASH in which all known resonances and the experimentally known cross sections, most importantly $\pi d \rightarrow \pi np$ and its inverse reaction, are included.

In this model, the number of deuterons at the kinetic freezeout is independent from their primordial abundance at the Cooper-Frye hypersurface. It was found that even when their initial number is set to zero, the number of deuterons regenerated in the hadronic phase converges towards the equilibrium value, which is the same as that predicted by the statistical hadronization model. Considering that in this

model only $\sim 1\%$ of the primordial deuterons survive the hadronic stage, the elliptic flow of deuterons observed after the kinetic freezeout is almost identical to that of the regenerated ones. For this reason, deuterons are not sampled at the Cooper-Frye hypersurface for these predictions.

The model predictions are consistent with the measured v_2 within the uncertainties in the centrality intervals 20–30% and 30–40% for $0.8 < p_T < 4$ GeV/c, while the data are overestimated by up to 30% in the centrality interval 10–20% for $p_T > 2$ GeV/c.
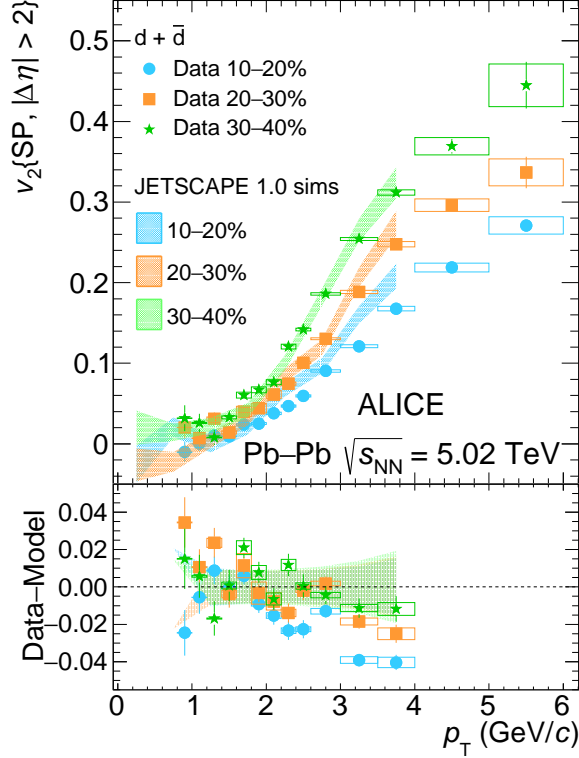
Figure 12: Measured deuterons v_2 compared to the predictions from a microscopic model [5] based on the JETSCAPE generator [52]. The model predictions, based on SMASH afterburner and which used TRENTo [51] initial conditions, are shown as bands. The width of the band represents the statistical uncertainty associated with the model. In the lower panel the data-to-model differences are shown. Vertical bars and boxes represent the statistical and systematic uncertainties, respectively.

5   Summary

The measurements of the deuterons v_2 and the first measurement of v_3 in Pb–Pb collisions at $\sqrt{s_{NN}} =$ 5.02 TeV are presented. The observed centrality and p_T dependence are consistent with the expectations from relativistic hydrodynamics. A mass ordering is observed for $p_T < 3$ GeV/c when comparing these results with the measured v_2 and v_3 of pions, kaons, and protons. The shift of the deuterons v_2 towards higher p_T with respect to the measurement in Pb–Pb collisions at $\sqrt{s_{NN}} = 2.76$ TeV, mainly due to a stronger radial flow at higher center-of-mass energy, is consistent with that observed for the proton v_2 measurement.

The results of this measurement are compared with the expectations from the simple coalescence approach, in which the deuterons v_2 is obtained from that of protons assuming that the deuterons invariant yield is proportional to that of protons squared, and with the predictions of the blast-wave model. The deuterons v_2 is overestimated by a simple coalescence approach, which describes the data only in periph-

eral (centrality > 50%) collisions. On the other hand, the blast-wave model underestimates the peripheral measurements and it is close to the data in central collisions. These results are consistent with the scenario previously seen for deuterons and ^{3}He elliptic flow: these simplified models bracket a region where the light nuclei v_2 is located and describe reasonably the data in different multiplicity regimes, indicating that none of these two models is able to describe the deuterons production measurement from low to high multiplicity environments.

Similar considerations are valid for the deuterons v_3 with some limitations due to the rather large statistical uncertainties. This specific aspect will be addressed with the larger data sample that will be collected in Run 3 following the ALICE upgrade, where a significant improvement of the statistical precision is expected. This measurement will be crucial to better constrain models that describe the production of light nuclei in heavy-ion collisions.

A more advanced coalescence model coupled to hydrodynamics and the hadronic afterburner UrQMD, which takes into account the quantum-mechanical properties of nucleons and nuclei and space-momentum correlations of nucleons, provides a good description of the deuterons v_2 and v_3 for $p_T > 2.5$ GeV/c. The model predictions deviate from the data at lower p_T, in particular for the centrality interval 10–20%. The same model provides a good description of the deuterons v_2 measured in Pb–Pb collisions at $\sqrt{s_{NN}} = 2.76$ TeV and that of ^{3}He at $\sqrt{s_{NN}} = 5.02$ TeV. The deuterons v_2 is also compared to the predictions from a hybrid model based on relativistic hydrodynamics coupled to the hadronic afterburner SMASH. The model predictions are consistent with the data within the uncertainties in the centrality intervals 20–30% and 30–40%, while a deviation of up to 30% is observed in the centrality interval 10–20% for $2 < p_T < 3$ GeV/c.

In general, the state-of-the-art implementations of coalescence and the hybrid approach based on hydrodynamics coupled to hadronic afterburners provide better descriptions of the data compared to the simple coalescence and blast-wave models. Further efforts, both on experimental and theoretical side, are needed to have a more comprehensive understanding of dynamics and production of light nuclei.

Acknowledgements

References

[1] A. Andronic, P. Braun-Munzinger, K. Redlich, and J. Stachel, "Decoding the phase structure of QCD via particle production at high energy", *Nature* **561** (2018) 321–330, arXiv:1710.09425 [nucl-th].

[2] V. Vovchenko and H. Stöcker, "Examination of the sensitivity of the thermal fits to heavy-ion hadron yield data to the modeling of the eigenvolume interactions", *Phys. Rev.* **C95** (2017) 044904, arXiv:1606.06218 [hep-ph].

[3] A. Andronic, P. Braun-Munzinger, J. Stachel, and H. Stöcker, "Production of light nuclei, hypernuclei and their antiparticles in relativistic nuclear collisions", *Phys. Lett.* **B697** (2011) 203–207, arXiv:1010.2995 [nucl-th].

[4] W. Zhao, L. Zhu, H. Zheng, C. M. Ko, and H. Song, "Spectra and flow of light nuclei in relativistic heavy ion collisions at energies available at the BNL Relativistic Heavy Ion Collider and at the CERN Large Hadron Collider", *Phys. Rev.* **C98** (2018) 054905, arXiv:1807.02813 [nucl-th].

[5] D. Oliinychenko, L.-G. Pang, H. Elfner, and V. Koch, "Microscopic study of deuteron production in Pb–Pb collisions at $\sqrt{s_{NN}}$ = 2.76 TeV via hydrodynamics and a hadronic afterburner", *Phys. Rev.* **C99** no. 4, (2019) 044907, arXiv:1809.03071 [hep-ph].

[6] **ALICE** Collaboration, S. Acharya *et al.*, "Evidence of rescattering effect in Pb–Pb collisions at the LHC through production of K*(892)^0 and ϕ(1020) mesons", *Phys. Lett.* **B802** (2020) 135225, arXiv:1910.14419 [nucl-ex].

[7] **ALICE** Collaboration, B. Abelev *et al.*, "Production of charged pions, kaons and protons at large transverse momenta in pp and Pb–Pb collisions at $\sqrt{s_{NN}}$ =2.76 TeV", *Phys. Lett.* **B736** (2014) 196–207, arXiv:1401.1250 [nucl-ex].

[8] **ALICE** Collaboration, S. Acharya *et al.*, "Production of charged pions, kaons, and (anti-)protons in Pb-Pb and inelastic pp collisions at $\sqrt{s_{NN}}$ = 5.02 TeV", *Phys. Rev. C* **101** no. 4, (2020) 044907, arXiv:1910.07678 [nucl-ex].

[9] N. Sharma, J. Cleymans, B. Hippolyte, and M. Paradza, "A Comparison of p-p, p-Pb, Pb–Pb Collisions in the Thermal Model: Multiplicity Dependence of Thermal Parameters", *Phys. Rev.* **C99** (2019) 044914, arXiv:1811.00399 [hep-ph].

[10] F. Becattini, E. Grossi, M. Bleicher, J. Steinheimer, and R. Stock, "Centrality dependence of hadronization and chemical freeze-out conditions in heavy ion collisions at $\sqrt{s_{NN}}$ = 2.76 TeV", *Phys. Rev.* **C90** (2014) 054907, arXiv:1405.0710 [nucl-th].

[11] **ALICE** Collaboration, S. Acharya *et al.*, "Production of ^{4}He and $^4\overline{\text{He}}$ in Pb–Pb collisions at $\sqrt{s_{NN}}$ = 2.76 TeV at the LHC", *Nucl. Phys.* **A971** (2018) 1–20, arXiv:1710.07531 [nucl-ex].

[12] S. T. Butler and C. A. Pearson, "Deuterons from High-Energy Proton Bombardment of Matter", *Phys. Rev.* **129** (1963) 836–842.

[13] J. I. Kapusta, "Mechanisms for deuteron production in relativistic nuclear collisions", *Phys. Rev.* **C21** (1980) 1301–1310. https://link.aps.org/doi/10.1103/PhysRevC.21.1301.

[14] R. Scheibl and U. W. Heinz, "Coalescence and flow in ultrarelativistic heavy ion collisions", *Phys. Rev.* **C59** (1999) 1585–1602, arXiv:nucl-th/9809092 [nucl-th].

[15] F. Cooper and G. Frye, "Single-particle distribution in the hydrodynamic and statistical thermodynamic models of multiparticle production", *Phys. Rev. D* **10** (Jul, 1974) 186–189. https://link.aps.org/doi/10.1103/PhysRevD.10.186.

[16] S. A. Bass *et al.*, "Microscopic models for ultrarelativistic heavy ion collisions", *Prog. Part. Nucl. Phys.* **41** (1998) 255–369, arXiv:nucl-th/9803035 [nucl-th].

[17] M. Bleicher *et al.*, "Relativistic hadron hadron collisions in the ultrarelativistic quantum molecular dynamics model", *J. Phys.* **G25** (1999) 1859–1896, arXiv:hep-ph/9909407 [hep-ph].

[18] **ALICE** Collaboration, S. Acharya *et al.*, "Measurement of deuteron spectra and elliptic flow in Pb–Pb collisions at $\sqrt{s_{NN}}$ = 2.76 TeV at the LHC", *Eur. Phys. J.* **C77** (2017) 658, arXiv:1707.07304 [nucl-ex].

[19] **ALICE** Collaboration, S. Acharya *et al.*, "Measurement of the (anti-)^{3}He elliptic flow in Pb-Pb collisions at $\sqrt{s_{NN}}$ = 5.02 TeV", *Phys. Lett. B* **805** (2020) 135414, arXiv:1910.09718 [nucl-ex].

[20] V. Vovchenko, K. Gallmeister, J. Schaffner-Bielich, and C. Greiner, "Nucleosynthesis in heavy-ion collisions at the LHC via the Saha equation", *Physics Letters B* **800** (2020) 135131, arXiv:1903.10024 [hep-ph].

[21] **ALICE** Collaboration, B. Abelev *et al.*, "Elliptic flow of identified hadrons in Pb–Pb collisions at $\sqrt{s_{NN}} = 2.76$ TeV", *JHEP* **06** (2015) 190, `arXiv:1405.4632 [nucl-ex]`.

[22] E. Schnedermann, J. Sollfrank, and U. W. Heinz, "Thermal phenomenology of hadrons from 200-A/GeV S+S collisions", *Phys. Rev.* **C48** (1993) 2462–2475, `arXiv:nucl-th/9307020 [nucl-th]`.

[23] **ALICE** Collaboration, B. Abelev *et al.*, "Performance of the ALICE Experiment at the CERN LHC", *Int. J. Mod. Phys.* **A29** (2014) 1430044, `arXiv:1402.4476 [nucl-ex]`.

[24] **ALICE** Collaboration, E. Abbas *et al.*, "Performance of the ALICE VZERO system", *JINST* **8** (2013) P10016, `arXiv:1306.3130 [nucl-ex]`.

[25] **ALICE** Collaboration, K. Aamodt *et al.*, "Centrality dependence of the charged-particle multiplicity density at mid-rapidity in Pb–Pb collisions at $\sqrt{s_{NN}} = 2.76$ TeV", *Phys. Rev. Lett.* **106** (2011) 032301, `arXiv:1012.1657 [nucl-ex]`.

[26] **ALICE** Collaboration, B. Abelev *et al.*, "Centrality determination of Pb–Pb collisions at $\sqrt{s} = 2.76$ TeV with ALICE", *Phys. Rev.* **C88** (2013) 044909, `arXiv:1301.4361 [nucl-ex]`.

[27] **ALICE** Collaboration, S. Acharya *et al.*, "Centrality determination in heavy ion collisions",. `https://cds.cern.ch/record/2636623`.

[28] **ALICE** Collaboration, K. Aamodt *et al.*, "Alignment of the ALICE Inner Tracking System with cosmic-ray tracks", *JINST* **5** (2010) P03003, `arXiv:1001.0502 [physics.ins-det]`.

[29] A. Akindinov *et al.*, "Performance of the ALICE Time-Of-Flight detector at the LHC", *Eur. Phys. J. Plus* **128** (2013) 44.

[30] **Particle Data Group** Collaboration, M. Tanabashi *et al.*, "Review of particle physics", *Phys. Rev. D* **98** (Aug, 2018) 030001. `https://link.aps.org/doi/10.1103/PhysRevD.98.030001`.

[31] **ALICE** Collaboration, J. Adam *et al.*, "Production of light nuclei and anti-nuclei in pp and Pb–Pb collisions at energies available at the CERN Large Hadron Collider", *Phys. Rev.* **C93** no. 2, (2016) 024917, `arXiv:1506.08951 [nucl-ex]`.

[32] S. A. Voloshin, A. M. Poskanzer, and R. Snellings, "Collective phenomena in non-central nuclear collisions", *Landolt-Bornstein* **23** (2010) 293–333, `arXiv:0809.2949 [nucl-ex]`.

[33] J.-Y. Ollitrault, A. M. Poskanzer, and S. A. Voloshin, "Effect of flow fluctuations and nonflow on elliptic flow methods", *Phys. Rev.* **C80** (2009) 014904, `arXiv:0904.2315 [nucl-ex]`.

[34] B. Alver and G. Roland, "Collision geometry fluctuations and triangular flow in heavy-ion collisions", *Phys. Rev.* **C81** (2010) 054905, `arXiv:1003.0194 [nucl-th]`. [Erratum: Phys. Rev.C82,039903(2010)].

[35] Z. Qiu and U. W. Heinz, "Event-by-event shape and flow fluctuations of relativistic heavy-ion collision fireballs", *Phys. Rev.* **C84** (2011) 024911, `arXiv:1104.0650 [nucl-th]`.

[36] R. S. Bhalerao and J.-Y. Ollitrault, "Eccentricity fluctuations and elliptic flow at RHIC", *Phys. Lett.* **B641** (2006) 260–264, `arXiv:nucl-th/0607009 [nucl-th]`.

[37] B. H. Alver, C. Gombeaud, M. Luzum, and J.-Y. Ollitrault, "Triangular flow in hydrodynamics and transport theory", *Phys. Rev.* **C82** (2010) 034913, `arXiv:1007.5469 [nucl-th]`.

[38] **ALICE** Collaboration, K. Aamodt *et al.*, "Higher harmonic anisotropic flow measurements of charged particles in Pb-Pb collisions at $\sqrt{s_{NN}}$=2.76 TeV", *Phys. Rev. Lett.* **107** (2011) 032301, `arXiv:1105.3865 [nucl-ex]`.

[39] **STAR** Collaboration, C. Adler *et al.*, "Elliptic flow from two and four particle correlations in Au+Au collisions at s(NN)**(1/2) = 130-GeV", *Phys. Rev.* **C66** (2002) 034904, `arXiv:nucl-ex/0206001 [nucl-ex]`.

[40] R. Barlow, "Systematic errors: Facts and fictions", in *Advanced Statistical Techniques in Particle Physics. Proceedings, Conference, Durham, UK, March 18-22, 2002*, pp. 134–144. 2002. `arXiv:hep-ex/0207026 [hep-ex]`. `http://www.ippp.dur.ac.uk/Workshops/02/statistics/proceedings//barlow.pdf`.

[41] S. Jeon and U. Heinz, "Introduction to Hydrodynamics", *Int. J. Mod. Phys.* **E24** (2015) 1530010, `arXiv:1503.03931 [hep-ph]`.

[42] **ALICE** Collaboration, J. Adam *et al.*, "Higher harmonic flow coefficients of identified hadrons in Pb-Pb collisions at $\sqrt{s_{NN}}$ = 2.76 TeV", *JHEP* **09** (2016) 164, `arXiv:1606.06057 [nucl-ex]`.

[43] **ALICE** Collaboration, S. Acharya *et al.*, "Anisotropic flow of identified particles in Pb–Pb collisions at $\sqrt{s_{NN}}$ = 5.02 TeV", *JHEP* **09** (2018) 006, `arXiv:1805.04390 [nucl-ex]`.

[44] **ALICE** Collaboration, J. Adam *et al.*, "Preliminary Physics Summary: Deuteron and anti-deuteron production in pp collisions at $\sqrt{s}$ = 13 TeV and in Pb–Pb collisions at $\sqrt{s_{NN}}$ = 5.02 TeV ",. `https://cds.cern.ch/record/2272148`.

[45] P. Huovinen, P. F. Kolb, U. W. Heinz, P. V. Ruuskanen, and S. A. Voloshin, "Radial and elliptic flow at RHIC: Further predictions", *Phys. Lett.* **B503** (2001) 58–64, `arXiv:hep-ph/0101136 [hep-ph]`.

[46] C. Shen, U. Heinz, P. Huovinen, and H. Song, "Radial and elliptic flow in Pb+Pb collisions at the Large Hadron Collider from viscous hydrodynamic", *Phys. Rev.* **C84** (2011) 044903, `arXiv:1105.3226 [nucl-th]`.

[47] **STAR** Collaboration, C. Adler *et al.*, "Identified particle elliptic flow in Au + Au collisions at $\sqrt{s_{NN}}$ = 130 GeV", *Phys. Rev. Lett.* **87** (2001) 182301, `arXiv:nucl-ex/0107003 [nucl-ex]`.

[48] P. J. Siemens and J. O. Rasmussen, "Evidence for a blast wave from compressed nuclear matter", *Phys. Rev. Lett.* **42** (1979) 880–883. `https://link.aps.org/doi/10.1103/PhysRevLett.42.880`.

[49] D. Molnar and S. A. Voloshin, "Elliptic flow at large transverse momenta from quark coalescence", *Phys. Rev. Lett.* **91** (2003) 092301, `arXiv:nucl-th/0302014 [nucl-th]`.

[50] Z.-W. Lin, C. M. Ko, B.-A. Li, B. Zhang, and S. Pal, "A Multi-phase transport model for relativistic heavy ion collisions", *Phys. Rev.* **C72** (2005) 064901, `arXiv:nucl-th/0411110 [nucl-th]`.

[51] J. S. Moreland, J. E. Bernhard, and S. A. Bass, "Alternative ansatz to wounded nucleon and binary collision scaling in high-energy nuclear collisions", *Phys. Rev.* **C92** no. 1, (2015) 011901, `arXiv:1412.4708 [nucl-th]`.

[52] **JETSCAPE** Collaboration, K. Kauder, "JETSCAPE v1.0 Quickstart Guide", *Nucl. Phys.* **A982** (2019) 615–618, `arXiv:1807.09615 [hep-ph]`.

[53] **PHENIX** Collaboration, S. S. Adler *et al.*, "Identified charged particle spectra and yields in au+au collisions at $\sqrt{s_{NN}}$ = 200 gev", *Phys. Rev. C* **69** (Mar, 2004) 034909. https://link.aps.org/doi/10.1103/PhysRevC.69.034909.

[54] **STAR** Collaboration, J. Adams *et al.*, "Identified particle distributions in pp and Au+Au collisions at $\sqrt{s_{NN}}$ = 200 GeV", *Phys. Rev. Lett.* **92** (2004) 112301, arXiv:nucl-ex/0310004 [nucl-ex].

[55] **STAR** Collaboration, J. Adams *et al.*, "Azimuthal anisotropy in Au+Au collisions at $\sqrt{s_{NN}}$ = 200 GeV", *Phys. Rev.* **C72** (2005) 014904, arXiv:nucl-ex/0409033 [nucl-ex].

A The ALICE Collaboration

S. Acharya[141] , D. Adamová[95] , A. Adler[74] , J. Adolfsson[81] , M.M. Aggarwal[100] , G. Aglieri Rinella[34] ,
M. Agnello[30] , N. Agrawal[10 ,54] , Z. Ahammed[141] , S. Ahmad[16] , S.U. Ahn[76] , Z. Akbar[51] , A. Akindinov[92] ,
M. Al-Turany[107] , S.N. Alam[40 ,141] , D.S.D. Albuquerque[122] , D. Aleksandrov[88] , B. Alessandro[59] ,
H.M. Alfanda[6] , R. Alfaro Molina[71] , B. Ali[16] , Y. Ali[14] , A. Alici[10 ,26 ,54] , N. Alizadehvandchali[125] ,
A. Alkin[2 ,34] , J. Alme[21] , T. Alt[68] , L. Altenkamper[21] , I. Altsybeev[113] , M.N. Anaam[6] , C. Andrei[48] ,
D. Andreou[34] , A. Andronic[144] , M. Angeletti[34] , V. Anguelov[104] , C. Anson[15] , T. Antičić[108] , F. Antinori[57] ,
P. Antonioli[54] , N. Apadula[80] , L. Aphecetche[115] , H. Appelshäuser[68] , S. Arcelli[26] , R. Arnaldi[59] , M. Arratia[80] ,
I.C. Arsene[20] , M. Arslandok[104] , A. Augustinus[34] , R. Averbeck[107] , S. Aziz[78] , M.D. Azmi[16] , A. Badalà[56] ,
Y.W. Baek[41] , S. Bagnasco[59] , X. Bai[107] , R. Bailhache[68] , R. Bala[101] , A. Balbino[30] , A. Baldisseri[137] , M. Ball[43] ,
S. Balouza[105] , D. Banerjee[3] , R. Barbera[27] , L. Barioglio[25] , G.G. Barnaföldi[145] , L.S. Barnby[94] , V. Barret[134] ,
P. Bartalini[6] , C. Bartels[127] , K. Barth[34] , E. Bartsch[68] , F. Baruffaldi[28] , N. Bastid[134] , S. Basu[143] , G. Batigne[115] ,
B. Batyunya[75] , D. Bauri[49] , J.L. Bazo Alba[112] , I.G. Bearden[89] , C. Beattie[146] , C. Bedda[63] , I. Belikov[136] ,
A.D.C. Bell Hechavarria[144] , F. Bellini[34] , R. Bellwied[125] , V. Belyaev[93] , G. Bencedi[145] , S. Beole[25] ,
A. Bercuci[48] , Y. Berdnikov[98] , D. Berenyi[145] , R.A. Bertens[130] , D. Berzano[59] , M.G. Besoiu[67] , L. Betev[34] ,
A. Bhasin[101] , I.R. Bhat[101] , M.A. Bhat[3] , H. Bhatt[49] , B. Bhattacharjee[42] , A. Bianchi[25] , L. Bianchi[25] ,
N. Bianchi[52] , J. Bielčík[37] , J. Bielčíková[95] , A. Bilandzic[105] , G. Biro[145] , R. Biswas[3] , S. Biswas[3] , J.T. Blair[119] ,
D. Blau[88] , C. Blume[68] , G. Boca[139] , F. Bock[96] , A. Bogdanov[93] , S. Boi[23] , J. Bok[61] , L. Boldizsár[145] ,
A. Bolozdynya[93] , M. Bombara[38] , G. Bonomi[140] , H. Borel[137] , A. Borissov[93] , H. Bossi[146] , E. Botta[25] ,
L. Bratrud[68] , P. Braun-Munzinger[107] , M. Bregant[121] , M. Broz[37] , E. Bruna[59] , G.E. Bruno[33 ,106] ,
M.D. Buckland[127] , D. Budnikov[109] , H. Buesching[68] , S. Bufalino[30] , O. Bugnon[115] , P. Buhler[114] , P. Buncic[34] ,
Z. Buthelezi[72 ,131] , J.B. Butt[14] , S.A. Bysiak[118] , D. Caffarri[90] , A. Caliva[107] , E. Calvo Villar[112] ,
J.M.M. Camacho[120] , R.S. Camacho[45] , P. Camerini[24] , F.D.M. Canedo[121] , A.A. Capon[114] , F. Carnesecchi[26] ,
R. Caron[137] , J. Castillo Castellanos[137] , A.J. Castro[130] , E.A.R. Casula[55] , F. Catalano[30] , C. Ceballos Sanchez[75] ,
P. Chakraborty[49] , S. Chandra[141] , W. Chang[6] , S. Chapeland[34] , M. Chartier[127] , S. Chattopadhyay[141] ,
S. Chattopadhyay[110] , A. Chauvin[23] , C. Cheshkov[135] , B. Cheynis[135] , V. Chibante Barroso[34] ,
D.D. Chinellato[122] , S. Cho[61] , P. Chochula[34] , T. Chowdhury[134] , P. Christakoglou[90] , C.H. Christensen[89] ,
P. Christiansen[81] , T. Chujo[133] , C. Cicalo[55] , L. Cifarelli[10 ,26] , L.D. Cilladi[25] , F. Cindolo[54] , M.R. Ciupek[107] ,
G. Clai[54 ,ii] , J. Cleymans[124] , F. Colamaria[53] , D. Colella[53] , A. Collu[80] , M. Colocci[26] , M. Concas[59 ,iii] , G. Conesa
Balbastre[79] , Z. Conesa del Valle[78] , G. Contin[24 ,60] , J.G. Contreras[37] , T.M. Cormier[96] , Y. Corrales Morales[25] ,
P. Cortese[31] , M.R. Cosentino[123] , F. Costa[34] , S. Costanza[139] , P. Crochet[134] , E. Cuautle[69] , P. Cui[6] ,
L. Cunqueiro[96] , D. Dabrowski[142] , T. Dahms[105] , A. Dainese[57] , F.P.A. Damas[115 ,137] , M.C. Danisch[104] ,
A. Danu[67] , D. Das[110] , I. Das[110] , P. Das[86] , P. Das[3] , S. Das[3] , A. Dash[86] , S. Dash[49] , S. De[86] , A. De Caro[29] ,
G. de Cataldo[53] , J. de Cuveland[39] , A. De Falco[23] , D. De Gruttola[10] , N. De Marco[59] , S. De Pasquale[29] ,
S. Deb[50] , H.F. Degenhardt[121] , K.R. Deja[142] , A. Deloff[85] , S. Delsanto[25 ,131] , W. Deng[6] , P. Dhankher[49] , D. Di
Bari[33] , A. Di Mauro[34] , R.A. Diaz[8] , T. Dietel[124] , P. Dillenseger[68] , Y. Ding[6] , R. Divià[34] , D.U. Dixit[19] ,
Ø. Djuvsland[21] , U. Dmitrieva[62] , A. Dobrin[67] , B. Dönigus[68] , O. Dordic[20] , A.K. Dubey[141] , A. Dubla[90 ,107] ,
S. Dudi[100] , M. Dukhishyam[86] , P. Dupieux[134] , R.J. Ehlers[96] , V.N. Eikeland[21] , D. Elia[53] , B. Erazmus[115] ,
F. Erhardt[99] , A. Erokhin[113] , M.R. Ersdal[21] , B. Espagnon[78] , G. Eulisse[34] , D. Evans[111] , S. Evdokimov[91] ,
L. Fabbietti[105] , M. Faggin[28] , J. Faivre[79] , F. Fan[6] , A. Fantoni[52] , M. Fasel[96] , P. Fecchio[30] , A. Feliciello[59] ,
G. Feofilov[113] , A. Fernández Téllez[45] , A. Ferrero[137] , A. Ferretti[25] , A. Festanti[34] , V.J.G. Feuillard[104] ,
J. Figiel[118] , S. Filchagin[109] , D. Finogeev[62] , F.M. Fionda[21] , G. Fiorenza[53] , F. Flor[125] , A.N. Flores[119] ,
S. Foertsch[72] , P. Foka[107] , S. Fokin[88] , E. Fragiacomo[60] , U. Frankenfeld[107] , U. Fuchs[34] , C. Furget[79] , A. Furs[62] ,
M. Fusco Girard[29] , J.J. Gaardhøje[89] , M. Gagliardi[25] , A.M. Gago[112] , A. Gal[136] , C.D. Galvan[120] , P. Ganoti[84] ,
C. Garabatos[107] , J.R.A. Garcia[45] , E. Garcia-Solis[11] , K. Garg[115] , C. Gargiulo[34] , A. Garibli[87] , K. Garner[144] ,
P. Gasik[105 ,107] , E.F. Gauger[119] , M.B. Gay Ducati[70] , M. Germain[115] , J. Ghosh[110] , P. Ghosh[141] , S.K. Ghosh[3] ,
M. Giacalone[26] , P. Gianotti[52] , P. Giubellino[59 ,107] , P. Giubilato[28] , A.M.C. Glaenzer[137] , P. Glässel[104] , A. Gomez
Ramirez[74] , V. Gonzalez[107 ,143] , L.H. González-Trueba[71] , S. Gorbunov[39] , L. Görlich[118] , A. Goswami[49] ,
S. Gotovac[35] , V. Grabski[71] , L.K. Graczykowski[142] , K.L. Graham[111] , L. Greiner[80] , A. Grelli[63] , C. Grigoras[34] ,
V. Grigoriev[93] , A. Grigoryan[1] , S. Grigoryan[75] , O.S. Groettvik[21] , F. Grosa[30 ,59] , J.F. Grosse-Oetringhaus[34] ,
R. Grosso[107] , R. Guernane[79] , M. Guittiere[115] , K. Gulbrandsen[89] , T. Gunji[132] , A. Gupta[101] , R. Gupta[101] ,
I.B. Guzman[45] , R. Haake[146] , M.K. Habib[107] , C. Hadjidakis[78] , H. Hamagaki[82] , G. Hamar[145] , M. Hamid[6] ,
R. Hannigan[119] , M.R. Haque[63 ,86] , A. Harlenderova[107] , J.W. Harris[146] , A. Harton[11] , J.A. Hasenbichler[34] ,
H. Hassan[96] , Q.U. Hassan[14] , D. Hatzifotiadou[10 ,54] , P. Hauer[43] , L.B. Havener[146] , S. Hayashi[132] ,
S.T. Heckel[105] , E. Hellbär[68] , H. Helstrup[36] , A. Herghelegiu[48] , T. Herman[37] , E.G. Hernandez[45] , G. Herrera
Corral[9] , F. Herrmann[144] , K.F. Hetland[36] , H. Hillemanns[34] , C. Hills[127] , B. Hippolyte[136] , B. Hohlweger[105] ,

J. Honermann[144] , D. Horak[37] , A. Hornung[68] , S. Hornung[107] , R. Hosokawa[15 ,133] , P. Hristov[34] , C. Huang[78] ,
C. Hughes[130] , P. Huhn[68] , T.J. Humanic[97] , H. Hushnud[110] , L.A. Husova[144] , N. Hussain[42] , S.A. Hussain[14] ,
D. Hutter[39] , J.P. Iddon[34 ,127] , R. Ilkaev[109] , H. Ilyas[14] , M. Inaba[133] , G.M. Innocenti[34] , M. Ippolitov[88] ,
A. Isakov[95] , M.S. Islam[110] , M. Ivanov[107] , V. Ivanov[98] , V. Izucheev[91] , B. Jacak[80] , N. Jacazio[34 ,54] ,
P.M. Jacobs[80] , S. Jadlovska[117] , J. Jadlovsky[117] , S. Jaelani[63] , C. Jahnke[121] , M.J. Jakubowska[142] ,
M.A. Janik[142] , T. Janson[74] , M. Jercic[99] , O. Jevons[111] , M. Jin[125] , F. Jonas[96 ,144] , P.G. Jones[111] , J. Jung[68] ,
M. Jung[68] , A. Jusko[111] , P. Kalinak[64] , A. Kalweit[34] , V. Kaplin[93] , S. Kar[6] , A. Karasu Uysal[77] , D. Karatovic[99] ,
O. Karavichev[62] , T. Karavicheva[62] , P. Karczmarczyk[142] , E. Karpechev[62] , A. Kazantsev[88] , U. Kebschull[74] ,
R. Keidel[47] , M. Keil[34] , B. Ketzer[43] , Z. Khabanova[90] , A.M. Khan[6] , S. Khan[16] , A. Khanzadeev[98] ,
Y. Kharlov[91] , A. Khatun[16] , A. Khuntia[118] , B. Kileng[36] , B. Kim[61] , B. Kim[133] , D. Kim[147] , D.J. Kim[126] ,
E.J. Kim[73] , H. Kim[17] , J. Kim[147] , J.S. Kim[41] , J. Kim[104] , J. Kim[147] , J. Kim[73] , M. Kim[104] , S. Kim[18] ,
T. Kim[147] , T. Kim[147] , S. Kirsch[68] , I. Kisel[39] , S. Kiselev[92] , A. Kisiel[142] , J.L. Klay[5] , C. Klein[68] , J. Klein[34 ,59] ,
S. Klein[80] , C. Klein-Bösing[144] , M. Kleiner[68] , T. Klemenz[105] , A. Kluge[34] , M.L. Knichel[34] , A.G. Knospe[125] ,
C. Kobdaj[116] , M.K. Köhler[104] , T. Kollegger[107] , A. Kondratyev[75] , N. Kondratyeva[93] , E. Kondratyuk[91] ,
J. Konig[68] , S.A. Konigstorfer[105] , P.J. Konopka[34] , G. Kornakov[142] , L. Koska[117] , O. Kovalenko[85] ,
V. Kovalenko[113] , M. Kowalski[118] , I. Králik[64] , A. Kravčáková[38] , L. Kreis[107] , M. Krivda[64 ,111] , F. Krizek[95] ,
K. Krizkova Gajdosova[37] , M. Krüger[68] , E. Kryshen[98] , M. Krzewicki[39] , A.M. Kubera[97] , V. Kučera[34 ,61] ,
C. Kuhn[136] , P.G. Kuijer[90] , L. Kumar[100] , S. Kundu[86] , P. Kurashvili[85] , A. Kurepin[62] , A.B. Kurepin[62] ,
A. Kuryakin[109] , S. Kushpil[95] , J. Kvapil[111] , M.J. Kweon[61] , J.Y. Kwon[61] , Y. Kwon[147] , S.L. La Pointe[39] , P. La
Rocca[27] , Y.S. Lai[80] , M. Lamanna[34] , R. Langoy[129] , K. Lapidus[34] , A. Lardeux[20] , P. Larionov[52] , E. Laudi[34] ,
R. Lavicka[37] , T. Lazareva[113] , R. Lea[24] , L. Leardini[104] , J. Lee[133] , S. Lee[147] , S. Lehner[114] , J. Lehrbach[39] ,
R.C. Lemmon[94] , I. León Monzón[120] , E.D. Lesser[19] , M. Lettrich[34] , P. Lévai[145] , X. Li[12] , X.L. Li[6] , J. Lien[129] ,
R. Lietava[111] , B. Lim[17] , V. Lindenstruth[39] , A. Lindner[48] , C. Lippmann[107] , M.A. Lisa[97] , A. Liu[19] , J. Liu[127] ,
S. Liu[97] , W.J. Llope[143] , I.M. Lofnes[21] , V. Loginov[93] , C. Loizides[96] , P. Loncar[35] , J.A. Lopez[104] , X. Lopez[134] ,
E. López Torres[8] , J.R. Luhder[144] , M. Lunardon[28] , G. Luparello[60] , Y.G. Ma[40] , A. Maevskaya[62] , M. Mager[34] ,
S.M. Mahmood[20] , T. Mahmoud[43] , A. Maire[136] , R.D. Majka[146 ,i] , M. Malaev[98] , Q.W. Malik[20] , L. Malinina[75 ,iv] ,
D. Mal'Kevich[92] , P. Malzacher[107] , G. Mandaglio[32 ,56] , V. Manko[88] , F. Manso[134] , V. Manzari[53] , Y. Mao[6] ,
M. Marchisone[135] , J. Mareš[66] , G.V. Margagliotti[24] , A. Margotti[54] , A. Marín[107] , C. Markert[119] ,
M. Marquard[68] , C.D. Martin[24] , N.A. Martin[104] , P. Martinengo[34] , J.L. Martinez[125] , M.I. Martínez[45] ,
G. Martínez García[115] , S. Masciocchi[107] , M. Masera[25] , A. Masoni[55] , L. Massacrier[78] , E. Masson[115] ,
A. Mastroserio[53 ,138] , A.M. Mathis[105] , O. Matonoha[81] , P.F.T. Matuoka[121] , A. Matyja[118] , C. Mayer[118] ,
F. Mazzaschi[25] , M. Mazzilli[53] , M.A. Mazzoni[58] , A.F. Mechler[68] , F. Meddi[22] , Y. Melikyan[62 ,93] ,
A. Menchaca-Rocha[71] , C. Mengke[6] , E. Meninno[29 ,114] , A.S. Menon[125] , M. Meres[13] , S. Mhlanga[124] ,
Y. Miake[133] , L. Micheletti[25] , L.C. Migliorin[135] , D.L. Mihaylov[105] , K. Mikhaylov[75 ,92] , A.N. Mishra[69] ,
D. Miśkowiec[107] , A. Modak[3] , N. Mohammadi[34] , A.P. Mohanty[63] , B. Mohanty[86] , M. Mohisin Khan[16 ,v] ,
Z. Moravcova[89] , C. Mordasini[105] , D.A. Moreira De Godoy[144] , L.A.P. Moreno[45] , I. Morozov[62] , A. Morsch[34] ,
T. Mrnjavac[34] , V. Muccifora[52] , E. Mudnic[35] , D. Mühlheim[144] , S. Muhuri[141] , J.D. Mulligan[80] , A. Mulliri[23 ,55] ,
M.G. Munhoz[121] , R.H. Munzer[68] , H. Murakami[132] , S. Murray[124] , L. Musa[34] , J. Musinsky[64] , C.J. Myers[125] ,
J.W. Myrcha[142] , B. Naik[49] , R. Nair[85] , B.K. Nandi[49] , R. Nania[10 ,54] , E. Nappi[53] , M.U. Naru[14] ,
A.F. Nassirpour[81] , C. Nattrass[130] , R. Nayak[49] , T.K. Nayak[86] , S. Nazarenko[109] , A. Neagu[20] , R.A. Negrao De
Oliveira[68] , L. Nellen[69] , S.V. Nesbo[36] , G. Neskovic[39] , D. Nesterov[113] , L.T. Neumann[142] , B.S. Nielsen[89] ,
S. Nikolaev[88] , S. Nikulin[88] , V. Nikulin[98] , F. Noferini[10 ,54] , P. Nomokonov[75] , J. Norman[79 ,127] , N. Novitzky[133] ,
P. Nowakowski[142] , A. Nyanin[88] , J. Nystrand[21] , M. Ogino[82] , A. Ohlson[81] , J. Oleniacz[142] , A.C. Oliveira Da
Silva[130] , M.H. Oliver[146] , C. Oppedisano[59] , A. Ortiz Velasquez[69] , T. Osako[46] , A. Oskarsson[81] ,
J. Otwinowski[118] , K. Oyama[82] , Y. Pachmayer[104] , V. Pacik[89] , S. Padhan[49] , D. Pagano[140] , G. Paić[69] , J. Pan[143] ,
S. Panebianco[137] , P. Pareek[50 ,141] , J. Park[61] , J.E. Parkkila[126] , S. Parmar[100] , S.P. Pathak[125] , B. Paul[23] ,
J. Pazzini[140] , H. Pei[6] , T. Peitzmann[63] , X. Peng[6] , L.G. Pereira[70] , H. Pereira Da Costa[137] , D. Peresunko[88] ,
G.M. Perez[8] , S. Perrin[137] , Y. Pestov[4] , V. Petráček[37] , M. Petrovici[48] , R.P. Pezzi[70] , S. Piano[60] , M. Pikna[13] ,
P. Pillot[115] , O. Pinazza[34 ,54] , L. Pinsky[125] , C. Pinto[27] , S. Pisano[10 ,52] , D. Pistone[56] , M. Płoskoń[80] ,
M. Planinic[99] , F. Pliquett[68] , M.G. Poghosyan[96] , B. Polichtchouk[91] , N. Poljak[99] , A. Pop[48] ,
S. Porteboeuf-Houssais[134] , V. Pozdniakov[75] , S.K. Prasad[3] , R. Preghenella[54] , F. Prino[59] , C.A. Pruneau[143] ,
I. Pshenichnov[62] , M. Puccio[34] , J. Putschke[143] , S. Qiu[90] , L. Quaglia[25] , R.E. Quishpe[125] , S. Ragoni[111] ,
S. Raha[3] , S. Rajput[101] , J. Rak[126] , A. Rakotozafindrabe[137] , L. Ramello[31] , F. Rami[136] , S.A.R. Ramirez[45] ,
R. Raniwala[102] , S. Raniwala[102] , S.S. Räsänen[44] , R. Rath[50] , V. Ratza[43] , I. Ravasenga[90] , K.F. Read[96 ,130] ,
A.R. Redelbach[39] , K. Redlich[85 ,vi] , A. Rehman[21] , P. Reichelt[68] , F. Reidt[34] , X. Ren[6] , R. Renfordt[68] ,
Z. Rescakova[38] , K. Reygers[104] , A. Riabov[98] , V. Riabov[98] , T. Richert[81 ,89] , M. Richter[20] , P. Riedler[34] ,

W. Riegler[34], F. Riggi[27], C. Ristea[67], S.P. Rode[50], M. Rodríguez Cahuantzi[45], K. Røed[20], R. Rogalev[91], E. Rogochaya[75], D. Rohr[34], D. Röhrich[21], P.F. Rojas[45], P.S. Rokita[142], F. Ronchetti[52], A. Rosano[56], E.D. Rosas[69], K. Roslon[142], A. Rossi[28 ,57], A. Rotondi[139], A. Roy[50], P. Roy[110], O.V. Rueda[81], R. Rui[24], B. Rumyantsev[75], A. Rustamov[87], E. Ryabinkin[88], Y. Ryabov[98], A. Rybicki[118], H. Rytkonen[126], O.A.M. Saarimaki[44], R. Sadek[115], S. Sadhu[141], S. Sadovsky[91], K. Šafařík[37], S.K. Saha[141], B. Sahoo[49], P. Sahoo[49], R. Sahoo[50], S. Sahoo[65], P.K. Sahu[65], J. Saini[141], S. Sakai[133], S. Sambyal[101], V. Samsonov[93 ,98], D. Sarkar[143], N. Sarkar[141], P. Sarma[42], V.M. Sarti[105], M.H.P. Sas[63], E. Scapparone[54], J. Schambach[119], H.S. Scheid[68], C. Schiaua[48], R. Schicker[104], A. Schmah[104], C. Schmidt[107], H.R. Schmidt[103], M.O. Schmidt[104], M. Schmidt[103], N.V. Schmidt[68 ,96], A.R. Schmier[130], J. Schukraft[89], Y. Schutz[136], K. Schwarz[107], K. Schweda[107], G. Scioli[26], E. Scomparin[59], J.E. Seger[15], Y. Sekiguchi[132], D. Sekihata[132], I. Selyuzhenkov[93 ,107], S. Senyukov[136], D. Serebryakov[62], A. Sevcenco[67], A. Shabanov[62], A. Shabetai[115], R. Shahoyan[34], W. Shaikh[110], A. Shangaraev[91], A. Sharma[100], A. Sharma[101], H. Sharma[118], M. Sharma[101], N. Sharma[100], S. Sharma[101], O. Sheibani[125], K. Shigaki[46], M. Shimomura[83], S. Shirinkin[92], Q. Shou[40], Y. Sibiriak[88], S. Siddhanta[55], T. Siemiarczuk[85], D. Silvermyr[81], G. Simatovic[90], G. Simonetti[34], B. Singh[105], R. Singh[86], R. Singh[101], R. Singh[50], V.K. Singh[141], V. Singhal[141], T. Sinha[110], B. Sitar[13], M. Sitta[31], T.B. Skaali[20], M. Slupecki[44], N. Smirnov[146], R.J.M. Snellings[63], C. Soncco[112], J. Song[125], A. Songmoolnak[116], F. Soramel[28], S. Sorensen[130], I. Sputowska[118], J. Stachel[104], I. Stan[67], P.J. Steffanic[130], E. Stenlund[81], S.F. Stiefelmaier[104], D. Stocco[115], M.M. Storetvedt[36], L.D. Stritto[29], A.A.P. Suaide[121], T. Sugitate[46], C. Suire[78], M. Suleymanov[14], M. Suljic[34], R. Sultanov[92], M. Šumbera[95], V. Sumberia[101], S. Sumowidagdo[51], S. Swain[65], A. Szabo[13], I. Szarka[13], U. Tabassam[14], S.F. Taghavi[105], G. Taillepied[134], J. Takahashi[122], G.J. Tambave[21], S. Tang[6 ,134], M. Tarhini[115], M.G. Tarzila[48], A. Tauro[34], G. Tejeda Muñoz[45], A. Telesca[34], L. Terlizzi[25], C. Terrevoli[125], D. Thakur[50], S. Thakur[141], D. Thomas[119], F. Thoresen[89], R. Tieulent[135], A. Tikhonov[62], A.R. Timmins[125], A. Toia[68], N. Topilskaya[62], M. Toppi[52], F. Torales-Acosta[19], S.R. Torres[37], A. Trifiró[32 ,56], S. Tripathy[50 ,69], T. Tripathy[49], S. Trogolo[28], G. Trombetta[33], L. Tropp[38], V. Trubnikov[2], W.H. Trzaska[126], T.P. Trzcinski[142], B.A. Trzeciak[37 ,63], A. Tumkin[109], R. Turrisi[57], T.S. Tveter[20], K. Ullaland[21], E.N. Umaka[125], A. Uras[135], G.L. Usai[23], M. Vala[38], N. Valle[139], S. Vallero[59], N. van der Kolk[63], L.V.R. van Doremalen[63], M. van Leeuwen[63], P. Vande Vyvre[34], D. Varga[145], Z. Varga[145], M. Varga-Kofarago[145], A. Vargas[45], M. Vasileiou[84], A. Vasiliev[88], O. Vázquez Doce[105], V. Vechernin[113], E. Vercellin[25], S. Vergara Limón[45], L. Vermunt[63], R. Vernet[7], R. Vértesi[145], L. Vickovic[35], Z. Vilakazi[131], O. Villalobos Baillie[111], G. Vino[53], A. Vinogradov[88], T. Virgili[29], V. Vislavicius[89], A. Vodopyanov[75], B. Volkel[34], M.A. Völkl[103], K. Voloshin[92], S.A. Voloshin[143], G. Volpe[33], B. von Haller[34], I. Vorobyev[105], D. Voscek[117], J. Vrláková[38], B. Wagner[21], M. Weber[114], S.G. Weber[144], A. Wegrzynek[34], S.C. Wenzel[34], J.P. Wessels[144], J. Wiechula[68], J. Wikne[20], G. Wilk[85], J. Wilkinson[10], G.A. Willems[144], E. Willsher[111], B. Windelband[104], M. Winn[137], W.E. Witt[130], J.R. Wright[119], Y. Wu[128], R. Xu[6], S. Yalcin[77], Y. Yamaguchi[46], K. Yamakawa[46], S. Yang[21], S. Yano[137], Z. Yin[6], H. Yokoyama[63], I.-K. Yoo[17], J.H. Yoon[61], S. Yuan[21], A. Yuncu[104], V. Yurchenko[2], V. Zaccolo[24], A. Zaman[14], C. Zampolli[34], H.J.C. Zanoli[63], N. Zardoshti[34], A. Zarochentsev[113], P. Závada[66], N. Zaviyalov[109], H. Zbroszczyk[142], M. Zhalov[98], S. Zhang[40], X. Zhang[6], Z. Zhang[6], V. Zherebchevskii[113], Y. Zhi[12], D. Zhou[6], Y. Zhou[89], Z. Zhou[21], J. Zhu[6 ,107], Y. Zhu[6], A. Zichichi[10 ,26], G. Zinovjev[2], N. Zurlo[140],

Affiliation notes

[i] Deceased

[ii] Italian National Agency for New Technologies, Energy and Sustainable Economic Development (ENEA), Bologna, Italy

[iii] Dipartimento DET del Politecnico di Torino, Turin, Italy

[iv] M.V. Lomonosov Moscow State University, D.V. Skobeltsyn Institute of Nuclear, Physics, Moscow, Russia

[v] Department of Applied Physics, Aligarh Muslim University, Aligarh, India

[vi] Institute of Theoretical Physics, University of Wroclaw, Poland

Collaboration Institutes

[1] A.I. Alikhanyan National Science Laboratory (Yerevan Physics Institute) Foundation, Yerevan, Armenia

[2] Bogolyubov Institute for Theoretical Physics, National Academy of Sciences of Ukraine, Kiev, Ukraine

[3] Bose Institute, Department of Physics and Centre for Astroparticle Physics and Space Science (CAPSS), Kolkata, India

[4] Budker Institute for Nuclear Physics, Novosibirsk, Russia

[5] California Polytechnic State University, San Luis Obispo, California, United States
[6] Central China Normal University, Wuhan, China
[7] Centre de Calcul de l'IN2P3, Villeurbanne, Lyon, France
[8] Centro de Aplicaciones Tecnológicas y Desarrollo Nuclear (CEADEN), Havana, Cuba
[9] Centro de Investigación y de Estudios Avanzados (CINVESTAV), Mexico City and Mérida, Mexico
[10] Centro Fermi - Museo Storico della Fisica e Centro Studi e Ricerche "Enrico Fermi", Rome, Italy
[11] Chicago State University, Chicago, Illinois, United States
[12] China Institute of Atomic Energy, Beijing, China
[13] Comenius University Bratislava, Faculty of Mathematics, Physics and Informatics, Bratislava, Slovakia
[14] COMSATS University Islamabad, Islamabad, Pakistan
[15] Creighton University, Omaha, Nebraska, United States
[16] Department of Physics, Aligarh Muslim University, Aligarh, India
[17] Department of Physics, Pusan National University, Pusan, Republic of Korea
[18] Department of Physics, Sejong University, Seoul, Republic of Korea
[19] Department of Physics, University of California, Berkeley, California, United States
[20] Department of Physics, University of Oslo, Oslo, Norway
[21] Department of Physics and Technology, University of Bergen, Bergen, Norway
[22] Dipartimento di Fisica dell'Università 'La Sapienza' and Sezione INFN, Rome, Italy
[23] Dipartimento di Fisica dell'Università and Sezione INFN, Cagliari, Italy
[24] Dipartimento di Fisica dell'Università and Sezione INFN, Trieste, Italy
[25] Dipartimento di Fisica dell'Università and Sezione INFN, Turin, Italy
[26] Dipartimento di Fisica e Astronomia dell'Università and Sezione INFN, Bologna, Italy
[27] Dipartimento di Fisica e Astronomia dell'Università and Sezione INFN, Catania, Italy
[28] Dipartimento di Fisica e Astronomia dell'Università and Sezione INFN, Padova, Italy
[29] Dipartimento di Fisica 'E.R. Caianiello' dell'Università and Gruppo Collegato INFN, Salerno, Italy
[30] Dipartimento DISAT del Politecnico and Sezione INFN, Turin, Italy
[31] Dipartimento di Scienze e Innovazione Tecnologica dell'Università del Piemonte Orientale and INFN Sezione di Torino, Alessandria, Italy
[32] Dipartimento di Scienze MIFT, Università di Messina, Messina, Italy
[33] Dipartimento Interateneo di Fisica 'M. Merlin' and Sezione INFN, Bari, Italy
[34] European Organization for Nuclear Research (CERN), Geneva, Switzerland
[35] Faculty of Electrical Engineering, Mechanical Engineering and Naval Architecture, University of Split, Split, Croatia
[36] Faculty of Engineering and Science, Western Norway University of Applied Sciences, Bergen, Norway
[37] Faculty of Nuclear Sciences and Physical Engineering, Czech Technical University in Prague, Prague, Czech Republic
[38] Faculty of Science, P.J. Šafárik University, Košice, Slovakia
[39] Frankfurt Institute for Advanced Studies, Johann Wolfgang Goethe-Universität Frankfurt, Frankfurt, Germany
[40] Fudan University, Shanghai, China
[41] Gangneung-Wonju National University, Gangneung, Republic of Korea
[42] Gauhati University, Department of Physics, Guwahati, India
[43] Helmholtz-Institut für Strahlen- und Kernphysik, Rheinische Friedrich-Wilhelms-Universität Bonn, Bonn, Germany
[44] Helsinki Institute of Physics (HIP), Helsinki, Finland
[45] High Energy Physics Group, Universidad Autónoma de Puebla, Puebla, Mexico
[46] Hiroshima University, Hiroshima, Japan
[47] Hochschule Worms, Zentrum für Technologietransfer und Telekommunikation (ZTT), Worms, Germany
[48] Horia Hulubei National Institute of Physics and Nuclear Engineering, Bucharest, Romania
[49] Indian Institute of Technology Bombay (IIT), Mumbai, India
[50] Indian Institute of Technology Indore, Indore, India
[51] Indonesian Institute of Sciences, Jakarta, Indonesia
[52] INFN, Laboratori Nazionali di Frascati, Frascati, Italy
[53] INFN, Sezione di Bari, Bari, Italy
[54] INFN, Sezione di Bologna, Bologna, Italy
[55] INFN, Sezione di Cagliari, Cagliari, Italy

[56] INFN, Sezione di Catania, Catania, Italy
[57] INFN, Sezione di Padova, Padova, Italy
[58] INFN, Sezione di Roma, Rome, Italy
[59] INFN, Sezione di Torino, Turin, Italy
[60] INFN, Sezione di Trieste, Trieste, Italy
[61] Inha University, Incheon, Republic of Korea
[62] Institute for Nuclear Research, Academy of Sciences, Moscow, Russia
[63] Institute for Subatomic Physics, Utrecht University/Nikhef, Utrecht, Netherlands
[64] Institute of Experimental Physics, Slovak Academy of Sciences, Košice, Slovakia
[65] Institute of Physics, Homi Bhabha National Institute, Bhubaneswar, India
[66] Institute of Physics of the Czech Academy of Sciences, Prague, Czech Republic
[67] Institute of Space Science (ISS), Bucharest, Romania
[68] Institut für Kernphysik, Johann Wolfgang Goethe-Universität Frankfurt, Frankfurt, Germany
[69] Instituto de Ciencias Nucleares, Universidad Nacional Autónoma de México, Mexico City, Mexico
[70] Instituto de Física, Universidade Federal do Rio Grande do Sul (UFRGS), Porto Alegre, Brazil
[71] Instituto de Física, Universidad Nacional Autónoma de México, Mexico City, Mexico
[72] iThemba LABS, National Research Foundation, Somerset West, South Africa
[73] Jeonbuk National University, Jeonju, Republic of Korea
[74] Johann-Wolfgang-Goethe Universität Frankfurt Institut für Informatik, Fachbereich Informatik und Mathematik, Frankfurt, Germany
[75] Joint Institute for Nuclear Research (JINR), Dubna, Russia
[76] Korea Institute of Science and Technology Information, Daejeon, Republic of Korea
[77] KTO Karatay University, Konya, Turkey
[78] Laboratoire de Physique des 2 Infinis, Irène Joliot-Curie, Orsay, France
[79] Laboratoire de Physique Subatomique et de Cosmologie, Université Grenoble-Alpes, CNRS-IN2P3, Grenoble, France
[80] Lawrence Berkeley National Laboratory, Berkeley, California, United States
[81] Lund University Department of Physics, Division of Particle Physics, Lund, Sweden
[82] Nagasaki Institute of Applied Science, Nagasaki, Japan
[83] Nara Women's University (NWU), Nara, Japan
[84] National and Kapodistrian University of Athens, School of Science, Department of Physics , Athens, Greece
[85] National Centre for Nuclear Research, Warsaw, Poland
[86] National Institute of Science Education and Research, Homi Bhabha National Institute, Jatni, India
[87] National Nuclear Research Center, Baku, Azerbaijan
[88] National Research Centre Kurchatov Institute, Moscow, Russia
[89] Niels Bohr Institute, University of Copenhagen, Copenhagen, Denmark
[90] Nikhef, National institute for subatomic physics, Amsterdam, Netherlands
[91] NRC Kurchatov Institute IHEP, Protvino, Russia
[92] NRC «Kurchatov» Institute - ITEP, Moscow, Russia
[93] NRNU Moscow Engineering Physics Institute, Moscow, Russia
[94] Nuclear Physics Group, STFC Daresbury Laboratory, Daresbury, United Kingdom
[95] Nuclear Physics Institute of the Czech Academy of Sciences, Řež u Prahy, Czech Republic
[96] Oak Ridge National Laboratory, Oak Ridge, Tennessee, United States
[97] Ohio State University, Columbus, Ohio, United States
[98] Petersburg Nuclear Physics Institute, Gatchina, Russia
[99] Physics department, Faculty of science, University of Zagreb, Zagreb, Croatia
[100] Physics Department, Panjab University, Chandigarh, India
[101] Physics Department, University of Jammu, Jammu, India
[102] Physics Department, University of Rajasthan, Jaipur, India
[103] Physikalisches Institut, Eberhard-Karls-Universität Tübingen, Tübingen, Germany
[104] Physikalisches Institut, Ruprecht-Karls-Universität Heidelberg, Heidelberg, Germany
[105] Physik Department, Technische Universität München, Munich, Germany
[106] Politecnico di Bari, Bari, Italy
[107] Research Division and ExtreMe Matter Institute EMMI, GSI Helmholtzzentrum für Schwerionenforschung GmbH, Darmstadt, Germany

[108] Rudjer Bošković Institute, Zagreb, Croatia
[109] Russian Federal Nuclear Center (VNIIEF), Sarov, Russia
[110] Saha Institute of Nuclear Physics, Homi Bhabha National Institute, Kolkata, India
[111] School of Physics and Astronomy, University of Birmingham, Birmingham, United Kingdom
[112] Sección Física, Departamento de Ciencias, Pontificia Universidad Católica del Perú, Lima, Peru
[113] St. Petersburg State University, St. Petersburg, Russia
[114] Stefan Meyer Institut für Subatomare Physik (SMI), Vienna, Austria
[115] SUBATECH, IMT Atlantique, Université de Nantes, CNRS-IN2P3, Nantes, France
[116] Suranaree University of Technology, Nakhon Ratchasima, Thailand
[117] Technical University of Košice, Košice, Slovakia
[118] The Henryk Niewodniczanski Institute of Nuclear Physics, Polish Academy of Sciences, Cracow, Poland
[119] The University of Texas at Austin, Austin, Texas, United States
[120] Universidad Autónoma de Sinaloa, Culiacán, Mexico
[121] Universidade de São Paulo (USP), São Paulo, Brazil
[122] Universidade Estadual de Campinas (UNICAMP), Campinas, Brazil
[123] Universidade Federal do ABC, Santo Andre, Brazil
[124] University of Cape Town, Cape Town, South Africa
[125] University of Houston, Houston, Texas, United States
[126] University of Jyväskylä, Jyväskylä, Finland
[127] University of Liverpool, Liverpool, United Kingdom
[128] University of Science and Technology of China, Hefei, China
[129] University of South-Eastern Norway, Tonsberg, Norway
[130] University of Tennessee, Knoxville, Tennessee, United States
[131] University of the Witwatersrand, Johannesburg, South Africa
[132] University of Tokyo, Tokyo, Japan
[133] University of Tsukuba, Tsukuba, Japan
[134] Université Clermont Auvergne, CNRS/IN2P3, LPC, Clermont-Ferrand, France
[135] Université de Lyon, Université Lyon 1, CNRS/IN2P3, IPN-Lyon, Villeurbanne, Lyon, France
[136] Université de Strasbourg, CNRS, IPHC UMR 7178, F-67000 Strasbourg, France, Strasbourg, France
[137] Université Paris-Saclay Centre d'Etudes de Saclay (CEA), IRFU, Départment de Physique Nucléaire (DPhN), Saclay, France
[138] Università degli Studi di Foggia, Foggia, Italy
[139] Università degli Studi di Pavia, Pavia, Italy
[140] Università di Brescia, Brescia, Italy
[141] Variable Energy Cyclotron Centre, Homi Bhabha National Institute, Kolkata, India
[142] Warsaw University of Technology, Warsaw, Poland
[143] Wayne State University, Detroit, Michigan, United States
[144] Westfälische Wilhelms-Universität Münster, Institut für Kernphysik, Münster, Germany
[145] Wigner Research Centre for Physics, Budapest, Hungary
[146] Yale University, New Haven, Connecticut, United States
[147] Yonsei University, Seoul, Republic of Korea